



HAL
open science

Incorporating cascading effects analysis in the maintenance policy assessment of torrent check dams against torrential floods

Nour Chahrour, Christophe Bérenguer, Jean-Marc Tacnet

► **To cite this version:**

Nour Chahrour, Christophe Bérenguer, Jean-Marc Tacnet. Incorporating cascading effects analysis in the maintenance policy assessment of torrent check dams against torrential floods. *Reliability Engineering and System Safety*, 2024, 243 (March), pp.109875. 10.1016/j.res.2023.109875 . hal-04332010

HAL Id: hal-04332010

<https://hal.science/hal-04332010v1>

Submitted on 8 Dec 2023

HAL is a multi-disciplinary open access archive for the deposit and dissemination of scientific research documents, whether they are published or not. The documents may come from teaching and research institutions in France or abroad, or from public or private research centers.

L'archive ouverte pluridisciplinaire **HAL**, est destinée au dépôt et à la diffusion de documents scientifiques de niveau recherche, publiés ou non, émanant des établissements d'enseignement et de recherche français ou étrangers, des laboratoires publics ou privés.



Distributed under a Creative Commons Attribution - NonCommercial - NoDerivatives 4.0 International License

Incorporating Cascading Effects Analysis in the Maintenance Policy Assessment of Torrent Check Dams Against Torrential Floods

Nour Chahrour^{a,b,*}, Christophe Bérenguer^b and Jean-Marc Tacnet^a

^aUniv. Grenoble Alpes, INRAE, CNRS, IRD, Grenoble INP, IGE, 38000 Grenoble, France.

^bUniv. Grenoble Alpes, CNRS, Grenoble INP, GIPSA-lab, 38000 Grenoble, France.

ARTICLE INFO

Keywords:

check dams
failure dependencies
bidirectional interactions
deterioration process
stochastic modeling
maintenance decision-making
torrential floods

ABSTRACT


In mountainous regions, protection infrastructures designed to mitigate the impacts of torrential floods often consist of a complex system of several structural components (check dams). Over time, the efficacy of this system in protecting downstream assets diminishes as the structural components deteriorate. The extent of deterioration is influenced by the interdependencies between the failure modes of individual components, as well as those between multiple components of the system. Understanding and quantifying the chain of failure events, known as cascading effects, is a critical scientific challenge that remains largely unexplored. In this study, we propose a novel approach that employs physics-based models to examine the deterioration of a series of check dams over time, while considering failure dependencies and bidirectional interactions between consecutive dams. **The results obtained from this approach reveals that the absence of a downstream dam accelerates the deterioration rate of upstream dams, while its presence serves to stabilize them.** We further incorporate stochastic deterioration and maintenance processes using Stochastic Petri nets to support decision-making regarding maintenance actions for each dam, while also considering economic factors. **Strategies involving minor operations achieved cost-effectiveness and prolonged satisfactory performance of the dams, with notable impacts from upstream and downstream dam presence on maintenance costs.** We illustrate our approach using a case study of the Faucon torrent in France, where we model the deterioration of three consecutive check dams subjected to torrential floods over a period of 100 years.

1. Introduction

Torrential hazards such as floods, debris flows, and landslides, are very destructive. In French Alps, statistical analysis has shown an increased frequency of torrential hazards since 1970 (Einhorn et al., 2015). Indeed, a considerable number of recent recorded torrential events has resulted in severe direct (destruction) and indirect (infrastructure disruption) damage, which in turn led to enormous economic loss. In France, structural protection measures (e.g., check dams, debris retention dams, dykes) are revealed to be very efficient in providing protection against torrential hazards. Since they guarantee the safety of people and protect socio-economic issues, protection systems are considered critical infrastructures that should always withstand and operate efficiently. The complex and hidden dependencies between the operation, deterioration, and total failure of protection systems make it difficult for their managers to properly estimate their efficacy and make optimal management (e.g., maintenance) decisions.

Modeling and analyzing cascading effects across an infrastructure system is one of the most challenging issues in critical infrastructure management (Dueñas-Osorio and Vemuru, 2009; Ouyang, 2014; Sharma and Gardoni, 2022; Zhao et al., 2023). Cascading effects, also known as “domino effects” have emerged as a field of scientific research in recent years. They are defined as a chain of dependent events induced by cause-effect relationships (?). In other words, an initial event can trigger other events, which in turn trigger consequences of varying magnitudes and severity (Pescaroli and Alexander, 2016). Cascading effects are multidimensional and evolve constantly over time, making them complex and difficult to assess and analyze. While the probability of such events is low, their occurrence can lead to catastrophic consequences for different infrastructure systems, the environment, and society as a whole. This

*Corresponding author

 nour.chahrour@inrae.fr (N. Chahrour)

ORCID(s): 0000-0003-2982-3169 (N. Chahrour)

48 highlights the need to develop models and simulation tools that incorporate cascading effects analyses, enabling a
49 credible assessment of the inevitable and sometimes unforeseen chain of events that could occur due to an initial event.

50 Like any other critical infrastructure system, the partial or total destruction of protection structures would pose a
51 significant threat to society. Over their lifetime, protection structures can deteriorate due to the direct impact of the
52 hazards they resist or indirectly from geomorphic activity (e.g., erosion, deposition) that occurs after each event. As a
53 result, protection structures may experience various types of interdependent failure modes that can have local or distant
54 impacts on their ability to protect downstream elements at risk (Chahrour et al., 2021, 2022; Pol et al., 2023). Without
55 regular inspection and maintenance, their deterioration could lead to complete failure, increasing the risk posed by
56 natural hazards. However, the French State provides limited monetary budgets for the management of these structures,
57 forcing managers to establish priorities for maintenance and to distribute available budgetary resources effectively.
58 Several research studies have been dedicated to developing models for prioritizing maintenance actions, considering
59 budgetary constraints, across different types of structural systems including bridges, offshore platforms, flood defences,
60 and wind turbines (Barone and Frangopol, 2014; Chen and Mehrabani, 2019; Morato et al., 2022; Vieira et al., 2022;
61 Saleh et al., 2023; Li et al., 2023).

62 Until recently, the level of deterioration of protection structures in mountains is assessed through visual inspection
63 (Carladous et al., 2019). The primary sources of information used by managers for making decisions about maintenance
64 strategies are photographs and written reports provided by experts following inspection visits. While visual inspection
65 provides information about the type and level of deterioration in real-time, it only captures a specific moment in time,
66 limiting managers' ability to have a dynamic view of the structure's deterioration over its lifetime. Additionally, the
67 underlying physics behind deterioration mechanisms, triggers of deterioration and the dependencies between failure
68 modes cannot be detected or known during visual inspection. This missing information prevents decision-makers from
69 having a comprehensive understanding of the situation necessary for making optimal management decisions.

70 Chahrour et al. (2021) and Chahrour et al. (2022) were the first to deal with the dynamic behavior of torrent
71 protection structures when subjected to deterioration mechanisms and maintenance operations over their lifetime.
72 Their research specifically considered check dams and debris retention systems, which are critical types of protection
73 structures. The authors developed scenario-driven physics-based models to study the deterioration process of each
74 case when subjected to torrential floods and debris flows, respectively. They also developed a decision-aiding model
75 using stochastic Petri net tools (Aubry et al., 2016) to assess different maintenance strategies considering the total cost
76 of each strategy. However, the deterioration trajectories were obtained while only considering interactions between
77 different types of failures. In reality, protection structures do not function separately; they are grouped into an integrated
78 system of interdependent components. Each component's behavior depends on other components based on existing
79 bidirectional dependencies. For example, Chahrour et al. (2021) modeled the deterioration of a single cantilever check
80 dam while considering the evolution of scouring under the foundation of the dam after a series of clear water floods
81 and the loss in its external stability triggered due to the formation of a scour hole under its foundation. Nevertheless,
82 several check dams are implemented in series in the flow channel of the torrent aiming to participate collaboratively
83 in resisting torrential floods and protecting socio-economic issues. The presence of a dam upstream or downstream of
84 another dam can limit the deterioration of the latter, while partial or total failure of one dam can negatively influence
85 other consecutive dams. Therefore, a more comprehensive approach is needed to evaluate the efficacy of interconnected
86 check dams and to prioritize maintenance strategies.

87 This study aims to build upon and expand the work conducted by Chahrour et al. (2021) incorporating bidirectional
88 dependencies between check dams when modeling the deterioration of each individual dam. In fact, practitioners
89 possess valuable empirical knowledge regarding the existence of these dependencies, while the contribution in this
90 study lies in developing a model that objectively captures and quantifies these dependencies. This model serves as a
91 robust decision-making tool, offering an advantage over relying solely on empirical knowledge for decision support.
92 The primary objective is to consider a multi-component protection system composed of several dams and to model the
93 deterioration of each dam from a structural standpoint in two different situations: (1) the presence of other dams and
94 (2) the absence of other dams. To achieve this goal, a physics-based model will be developed to simulate the evolution
95 of selected degradation indicators, both dependent and independent, in each of the defined situations. Subsequently,
96 a decision-aiding model will be constructed using stochastic Petri nets (SPNs) to represent various maintenance
97 strategies. This model will assist in supporting maintenance decision-making within the check dam management
98 process.

99 [In the realm of enhancing safety and reliability in complex technological systems, this study contributes significantly by addressing the fundamental challenge of understanding and quantifying cascading effects within protection](#)
100

systems. It offers insights into the relative deterioration rates among check dam system components, emphasizing the interconnectedness and interdependencies between check dams. Leveraging Stochastic Petri Nets (SPNs), it integrates deterioration and maintenance processes, facilitating informed decision-making for maintenance actions, thereby ensuring a more reliable and effective approach to ensure the protection system's safety. Furthermore, it thoroughly explores a real case study to evaluate the effects of various maintenance strategies on the reliability of check dam systems, ultimately reducing uncertainty for decision-makers managing complex protection systems, a pivotal element in enhancing its safety and reliability. Indeed, by conducting such analyses, decision-makers will be able to effectively address key questions, such as the frequency of overall system inspections, the most crucial degradation indicators for diagnosis, which dam is the most critical and requires priority repair, optimal timing for maintenance actions and which specific maintenance operations should be employed considering the current level of degradation (minor, major, or corrective). The answers to the previous questions are the most necessary information required for optimizing maintenance strategies and respecting available budgets allocated to these systems.

This paper is organized as follows: Section 1 provides an overview of the general context, objectives, and main contributions behind this research. Section 2 offers a brief summary of the existing literature on cascading effects and the methods used to model this phenomenon in the context of natural hazards and torrent protection structures. Section 3 outlines the proposed methodology for modeling the deterioration of check dams and supporting maintenance decision-making while considering cascading effects. Section 4 presents a real case study, including the obtained results and corresponding discussions. Finally, Section 5 presents the general conclusions drawn from the study.

2. Cascading Effects Analysis in Torrential Risk Context

Torrents are mountain streams characterized by short and narrow valleys, steep slopes ($> 6\%$), and high geomorphic activity due to sediment transport (Bernard, 1925). Torrential watersheds frequently experience high-intensity precipitation events that are typically localized to small areas. Consequently, rapid and destructive flows, such as clear water floods and debris flows, are generated. These so-called torrential events are gravitational phenomena that propagate from the upstream to the downstream of the watershed. They have the capability to erode and destabilize banks, transport sediment, and deposit materials on fans and into the downstream main rivers. These processes are governed by the geomorphological dynamics and the topographic characteristics of the torrential watershed.

2.1. Check Dams in Torrential Watersheds

Torrential watersheds are composed of three main parts: the upstream receiving basin, the flow channel, and the downstream alluvial fan (fig. 1a). These components are associated with the processes of material production, transfer, and deposition (Surell, 1841). In France, check dams are the most commonly used type of protection structures in mountainous regions, with the majority of French torrents featuring over 100 check dams. Check dams are civil engineering structures (cantilever or gravity dams). Gravity check dams are generally composed of three main elements: a trapezoidal hydraulic spillway, a central body, and lateral wings (fig. 1c). They are often implemented in a series along the flow channel of a torrential watershed, with a specific distance separating them, (fig. 1b) to collaboratively achieve specific functions (fig. 1d), such as stabilizing longitudinal and transverse profiles, reducing the slope of the torrent bed, and redirecting the flow to minimize lateral erosion of banks (Piton et al., 2017). Although check dams resemble traditional retaining walls, they incorporate additional hydraulic functions. Therefore, their design typically involves two criteria (fig. 1e): classical structural analysis and functional analysis considering torrential hydraulics (Tacnet and Degoutte, 2013).

In the field of structural design for check dams, Deymier et al. (1995) has provided a technical reference document that adapts classical civil engineering stability justifications to the specific requirements of torrent protection structures, taking into account factors such as geotechnical characteristics and loading conditions. Throughout their lifespan, the efficacy of check dams gradually diminishes due to various types of potential failures. These failures manifest as indicators that emerge and evolve over time as a result of structural aging, geomorphic activity (such as deposition and erosion) occurring adjacent to or beneath the check dams, and the impact of torrential hazards on the structures. To ensure the safety and longevity of check dams, as well as to safeguard socio-economic interests, the French state has implemented a policy known as ONF-RTM (Office national des forêts - Restauration des terrains en montagne). This policy aims to propose protective measures, oversee their implementation across the country, and assess their long-term efficacy.

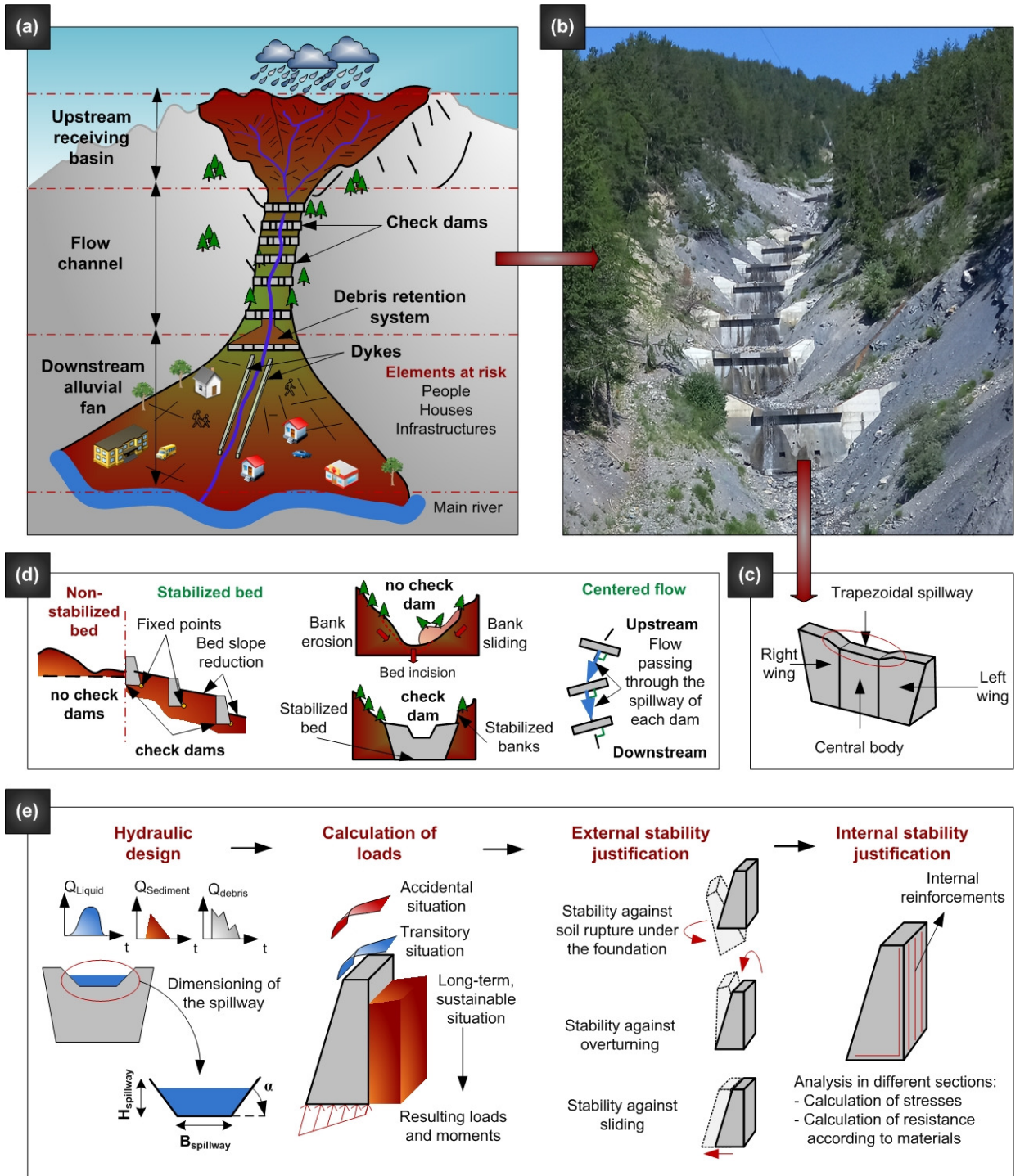


Figure 1: General context of torrent check dams: (a) illustration depicting the zones and elements involved in a protected torrential watershed; (b) series of check dams implemented in the flow channel of a torrential watershed, Faucon torrent, France © ONF-RTM 2022; (c) check dam's structural components; (e) structural analysis of a cantilever check dam.

150 As a part of natural risk assessment, the efficacy of protection structures should be assessed taking into
 151 consideration scenario analysis. While it may not be possible to completely prevent damages after natural hazards,

their accumulation can be mitigated by identifying the occurrence of both direct primary events (such as torrential phenomena) and indirect secondary events (their consequences) and understanding their interdependencies at early stages. These interdependencies play a crucial role in analyzing the actual behavior of the structures. Consequently, risk analysis cannot rely solely on assessing individual risk levels associated with independent events. It is essential to consider cascading effects and analyze the overall risk level by accounting for the interactions among all potential events. Although incorporating cascading effects increases the complexity of the analysis, conducting a multi-risk assessment that captures the interactions among different events is crucial for a comprehensive understanding of the risks involved.

2.2. Scenario Building for Risk Management

The assessment of how cascading effects exacerbate the failures of check dams, both in terms of direct and indirect damage, is a crucial aspect of managing torrential risks. Risk managers are faced with the challenge of not only mitigating the impact of the natural hazards themselves but also addressing the chain of failure events that protection structures experience during and after these hazardous events. By conducting a comprehensive assessment of cascading effects, decision-makers are better equipped to develop effective risk management strategies within the framework of prevention (e.g., risk assessment), preparedness (e.g., emergency planning), and recovery (e.g., maintenance).

Given that the study of cascading effects is a relatively new field in the context of natural and technological risks, there are limitations in existing methodologies and field experiences (Cheng et al., 2021; Mühlhofer et al., 2023). To assess the overall risk level associated with dependent and/or independent undesired events, it is necessary to define a risk scenario. This involves identifying the events that may be triggered following an initial event, as well as the potential consequences of each of these triggered events. A risk scenario represents a single or multiple risk situations and the paths leading to possible consequences. As a first step, these scenarios are often visualized in a compatibility/transition matrix, which makes it possible to build all possible chain of events triggered after an initial event (Gill and Malamud, 2014, 2016). This matrix serves as a theoretical modeling framework for cascading effect scenarios, which can then be further modeled using quantitative risk assessment approaches, such as event tree analysis, in which the transition probabilities between events are identified (Modarres, 1992).

In the literature, event trees (ETs) have emerged as the most commonly adopted methodological approach for analyzing cascading effects (Mineo et al., 2017; Misuri et al., 2021). However, a key limitation of ETs is their assumption of event independence, which means they do not account for events with joint probabilities occurring simultaneously. They also consider binary events, in which the failure of the system is not linked to physical modeling. These limitations hampers the ability of ETs to accurately model complex dependencies, leading to unreliable cascading effects scenarios at the local level. Consequently, decision-makers may not receive sufficient information for effective risk prevention and preparedness measures. Additionally, defining accurate transition probabilities is crucial for obtaining a reliable risk assessment. These probabilities are typically derived from historical databases, scientific literature reviews, or expert elicitation. However, the available information is often limited and accompanied by uncertainties, making full probabilistic modeling of cascading effects highly complex. To address these challenges and provide decision-makers with reliable inputs for simulation tools, it is essential to develop a comprehensive understanding of cascading effects scenarios at the local level. This involves considering dependent events that can occur simultaneously and quantifying the associated risk scenarios through physics-based modeling.

2.3. Dependencies Triggering Check Dam Failure

When managing torrential risk in the presence of protection structures, it is crucial for managers to consider the dependencies that can arise between different natural hazards (e.g., flood triggering landslides), failure modes of check dams (e.g., local scouring triggering loss in external stability), and components within a multi-component protection system (e.g., failure of one dam triggering failure of other consecutive dams). These dependencies can give rise to significant cascading effects. Figuring out such dependencies is essential to (i) better model the deterioration of check dams over time, (ii) have a robust assessment of their efficacy level, and (iii) choose the most appropriate maintenance strategy that have the efficiency to increase the availability time of the structures and therefore to reduce the risk level as much as possible.

Gill and Malamud (2014) developed a transition matrix that provides all the possible interactions between natural hazards of different nature (e.g., geophysical, hydrological, biophysical, etc.). However, to date, no study has specifically addressed the dependencies between different types of failures in check dams. Carladous (2017) defined various failure modes that check dams may experience throughout their lifespan, which can result from improper

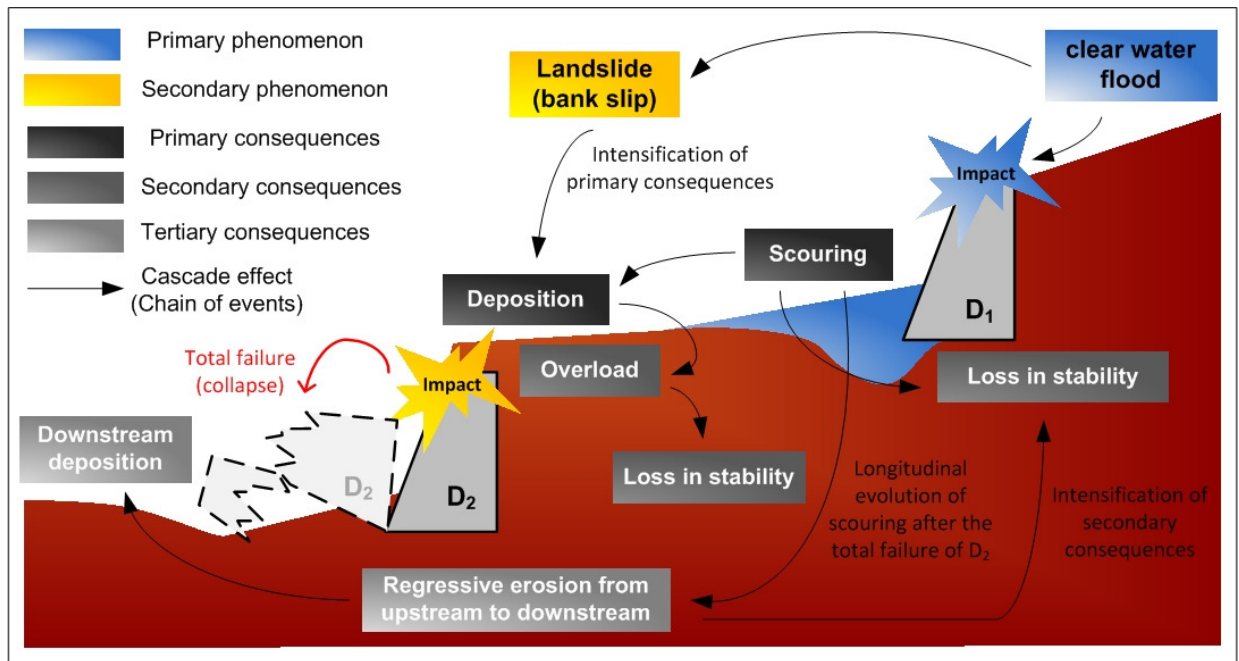


Figure 2: Illustration of cascading effects within a system of check dams triggered due to torrential hazards.

203 design or external accidents. Notably, the dependencies between these different failure modes have not been thoroughly
 204 investigated. A significant advancement in understanding the dependencies within check dams was made by Chahrour
 205 et al. (2021), who modeled the relationship between local scouring under the dam's foundation and its external stability.
 206 This study revealed that depending on the dimensions of the scour pit, the dam could experience total collapse due
 207 to overturning or soil rupture beneath its foundation. However, Chahrour et al. (2021) assumed that the behavior of a
 208 single check dam within a series of dams is independent of the behavior of other consecutive dams. This simplification
 209 does not fully capture the complex interdependencies that exist in reality.

210 Since they are located in series, check dams are part of an interdependent multi-component system that interacts
 211 with the torrent bed and lateral banks. The deterioration or failure of one specific component within a check dam
 212 (e.g., foundation, spillway) can trigger the total failure of the entire structure. This failure, in turn, may propagate
 213 to the upstream and downstream structures within the system through various mechanisms such as regressive upstream
 214 erosion or excessive downstream deposition. On one hand, the presence of one check dam can positively influence
 215 the behavior (e.g., deterioration rate) of other consecutive dams. On the other hand, the partial or total failure of
 216 one check dam may negatively impact the behavior of other consecutive dams. In summary, while progress has been
 217 made in understanding the dependencies within check dams, further research is needed to fully explore the complex
 218 interactions and interdependencies between different failure modes and consecutive dams.

219 As for critical infrastructures (CIs), the failure or disruption of one infrastructure can have cascading effects,
 220 potentially leading to partial or total failures in other interconnected infrastructures. Dependencies between CIs are
 221 usually categorized as physical, cyber, geographic, logical, and social dependencies (Rinaldi et al., 2001). In the case
 222 of torrent check dams, we mainly focus on physical, geographic, and social dependencies, as described below:

- 223 - Physical dependencies: arise when the state of one check dam is influenced by the material outputs (e.g., released
 224 volume of sediments) from another check dam within the system.
- 225 - Geographic dependencies: occur when the state of a check dam is influenced by an environmental event associated
 226 with another check dam due to their close proximity or spatial arrangement (e.g., failure propagation due to small
 227 distance separating the two dams).
- 228 - Social dependencies: are related to human activities surrounding the check dams (e.g., land use).

Figure 2 illustrates an example of cascading effect that showcases the various types of interactions and dependencies observed within the context of torrential hazards and check dams. It represents a multi-component system consisting of two check dams, namely D_1 and D_2 , with a specific distance between them. Initially, the system experiences a clear water flood as the primary hazard, resulting in primary consequences such as scouring downstream D_1 and deposition upstream D_2 . Additionally, this flood event triggers a landslide in one of the banks due to the saturation of bank materials with water. The primary consequences then give rise to secondary consequences, including the loss of stability in D_1 due to scouring (erosion of materials beneath the dam's base). Furthermore, the secondary hazard of the landslide possesses the potential to amplify the consequences stemming from the primary hazard. For instance, it can increase the volume of deposition and trigger the destruction of the dam underneath (e.g., D_2) due to overload. The total collapse of D_2 lead to tertiary consequences, such as the progressive evolution of scouring downstream D_2 due to the increase in the bed slope, which in turn increases the volume of deposition in downstream areas due to solid transport. Consequently, the figure reveals three possible cascading effects scenarios: (1) a torrential hazard triggering another hazard (flood triggering landslide); (2) one failure mode triggering another failure mode (scouring triggering loss in dam's stability); and (3) a failure in D_2 leading to a failure in D_1 (scouring downstream D_1 increases after the collapse of D_2).

In this study, our focus is specifically directed towards understanding the dependencies between check dams situated in a series configuration. We will explore how the state of each dam evolves over time considering the impacts of the torrential hazards on the dam itself as well as the physical and geographic interdependencies with other consecutive dams. The following section describes the methodology developed and used to address these challenges.

3. Developed Methodological Approach

This section presents our methodological contribution, which is divided into several subsections. The developed approach consists of three key sub-models. Firstly, we employ a torrential hydraulic model to simulate the behavior of the torrent bed in terms of erosion and deposition, when exposed to a series of clear water floods over time. Secondly, we develop a physics-based model to capture the dynamic deterioration of each individual dam within the system considering its loss in external stability. This model considers the influence of each flood event on the condition of the dam, accounting for the presence or absence of other dams in the system. Lastly, we introduce a decision-aiding model that supports maintenance decision-making for the check dam system. In the subsequent subsections, we provide a comprehensive description of each sub-model and its respective role within our integrated approach.

3.1. Torrential Hydraulic Numerical Modeling

In torrential watersheds, sediment transport plays a crucial role in shaping the morphology of the torrent (Recking et al., 2013). To understand and model the complex phenomena behind torrential hydraulics, specialized tools that can simulate both water flow and sediment transport along the torrent are required. While propagating from upstream to downstream, clear water floods have the potential to erode both the bed and banks of the torrent triggering slope destabilization. Furthermore, the large volume of transported sediments will be subsequently deposited, resulting in an elevated bed level and potentially leading to overflows. Ongoing efforts are focused on enhancing scientific knowledge and developing appropriate methods and tools to study torrential hydraulics and effectively manage associated risks.

Specific software, like LOGICCHAR, has been developed by Laigle (2008) to study these phenomena. It is a one-dimensional numerical model that predicts the evolution of the torrent's bed during torrential floods based on hypotheses and existing sediment transport laws. To launch simulations using LOGICCHAR, several input data parameters need to be provided. These include the geometric features of the torrent (longitudinal and transverse profiles), the protection system (location and observed height of the dams), the characteristics of the torrent bed (grain size distribution, depth of erodible layer), and the hydrographs of the flood events occurring over the period of simulation (duration, peak discharge, time to peak). In addition, the operator is required to define the scan points (both temporal and spatial) at which they wish to observe the corresponding outputs. Further details and illustrations of these input parameters can be found in fig. 3.

To model the evolution of the torrent bed and the subsequent behavior of the check dams over time, it is essential to generate and simulate flood events that could potentially occur throughout a specified period of time (e.g., 100 years). These series of flood events are referred to as "scenarios." To account for possible uncertainties, multiple scenarios of realistic flood events need to be generated. By considering the peak water discharge (Q_{peak}) and date of occurrence of the flood events as random variables, it is possible to generate as many scenarios as desired. Each scenario may

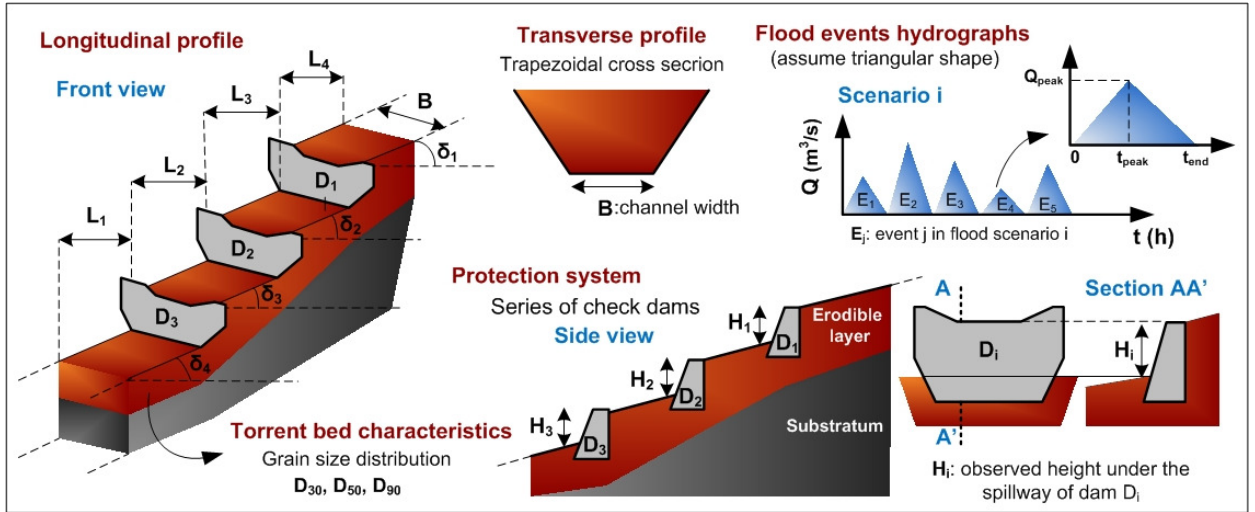


Figure 3: Input data for torrential hydraulic numerical simulations in LOGICCHAR.

279 encompass a different number of flood events, representing the potential occurrences during the specified simulation
 280 period. The choice of probability laws and their associated parameters used to create those random variables is based
 281 on available data and expert assumption. Expert knowledge can also be employed to depict the hydrograph of each
 282 event, including its shape, time to peak discharge t_{peak} , and duration t_{end} .

283 Each flood scenario, is inputted into LOGICCHAR as a whole and modeled separately from other scenarios. The
 284 scenario is represented as a set of hydrographs, each corresponding to a specific event within the scenario. Although
 285 each flood event within the scenario has a designated date of occurrence, LOGICCHAR does not require a time separation
 286 between consecutive events. This is because the torrent bed remains stable during this period of time. Based on all the
 287 input data, LOGICCHAR performs continuous calculations of the coupled hydraulics and sediment transport at every
 288 location along the simulated torrent bed throughout the entire duration of each flood event. After the simulation is
 289 completed, the results are presented in the form of graphs and tables. At each selected temporal scan point, the outputs
 290 consist of the water height (m), water velocity (m/s), slope (m/m), initial bed level (m), actual bed level (m), and solid
 291 discharge (m^3/s) along the entire length of the torrent. Similarly, for each chosen spatial scan point, the aforementioned
 292 outputs are provided for the entire duration of the flood event.

293 3.2. Check Dams' Stability Modeling

294 Over time, the external stability of the check dam is influenced by several factors including the direct impact of
 295 flood events and due to local scouring. The erosion of the bed materials downstream the dam creates a global scour
 296 pit, which keep on propagating with a given slope until reaching the based of the dam thus creating a local scour pit,
 297 characterized by the removal of solid materials under the structure thus removing the its support. The stability of the
 298 dam varies depending on the dimensions of the local scour pit. **In the context of check dams and their external stability,**
 299 **it is essential to consider how various factors directly impact the dimensions of scour pits.** These factors include the
 300 flow velocity and water volume, with higher values increasing erosive potential and leading to the formation of larger
 301 scour pits, especially in regions prone to heavy rainfall. Additionally, the amount of sediment carried by the water also
 302 plays a crucial role; when sediment loads exceed a dam's capacity, larger scour pits can result. Besides, the properties
 303 of the torrent bed, such as grain size distribution, cohesion, and friction angle, further affect the pit's dimensions. For
 304 instance, loose, fine sediments with little cohesion in the torrent bed can lead to deeper and wider scour pits. Engineers
 305 and designers must consider these site-specific factors to ensure the effectiveness of check dams in providing protection
 306 against erosion. It is also worth noting that clear water floods tend to result in larger ultimate scouring depths compared
 307 to other flow conditions (Prendergast and Gavin, 2014). Hence, this study specifically focuses on investigating the
 308 effects of clear water floods on the stability of the check dam.

3.2.1. Global and Local Scouring Estimation

Several methods have been developed to estimate the size of the global scour pit, which is an important factor in assessing the stability of check dams. Two commonly used, but older methods in this context of torrent protection structures are the Vawe and Sogreah methods (Couvert, B. et al., 1991). Vawe method is a two-dimensional model that calculates the depth and the length of the global scour pit. The sogreah method, an extension of Vawe, is a three-dimensional model that estimates the depth, length, and width of the global scour pit. Comiti et al. (2013) proposed a more recent approach based on laboratory experiments and field measurements, focusing on estimating the depth of the global scour pit. While the Sogreah method tends to overestimate the scour depth compared to the Comiti approach, it offers the advantage of calculating all three dimensions of the global scour pit. To address this, Chahrour et al. (2021) developed an integrated approach that combines the Sogreah and Comiti methods, providing reliable calculations of the three dimensions of the global scour pit. In this study, we will employ this integrated approach to assess the stability of check dams.

According to Chahrour et al. (2021), the depth P , width l , and length L of the global scour pit can be estimated using the following equations:

$$P = [S + h_s] \cdot R \quad (m) \quad (1)$$

$$l = [S + h_s] \cdot R' \quad (m) \quad (2)$$

$$L = [S + h_s] \cdot R'' \quad (m) \quad (3)$$

$$S = 2 \cdot Z \left(\frac{H_s}{Z} \right)^{0.59} \left(\frac{b}{B} \right)^{2.34} \left(\frac{\Delta D_{90}}{Z} \right)^{-0.09} \quad (m) \quad (4)$$

where S (m) corresponds to the maximum depth of erosion from the level of the initial torrent bed, h_s (m) is the downstream water level, Z (m) is the drop height, H_s (m) is the hydraulic head, b (m) is the base width of the dam's spillway, B (m) is the torrent channel width, Δ is the sediment relative submerged density, and D_{90} (m) is the grain size for which 90% of the bed material are finer by weight. R , R' , and R'' are correction coefficients that consider the three-dimensional effects associated with flow contraction. These coefficients are extracted from an abacus based on a dimensionless contraction coefficient C_c , which is calculated using the following equation (Couvert, B. et al., 1991):

$$C_c = \frac{H_s * h_c}{L_s^2} \quad (5)$$

where H_s (m), h_c (m), and L_s (m), given by the following equations, correspond respectively to the hydraulics head, the hydraulic drop, and the width of the spillway at the level of the water.

$$H_s = h + \frac{v^2}{2g}; \quad h_c = (H_{sp} + H_s) - (Z_F + h_s); \quad L_s = b + H_s$$

where h (m) is the upstream water level, v (m/s) is the water velocity, g (m^2/s) is the gravitational acceleration, H_{sp} (m) is the height of the dam under its spillway, Z_F (m) is the bed level after event i of the simulated flood scenario, which is calculated as the sum of Z_{FI} (m) and d_z (m) representing respectively the initial bed level and the drop between the bed levels.

The crucial parameters for assessing dam stability are the depth S_d (m) and the width S_w (m) of the local scour pit formed under the dam's base. S_w is equivalent to the length l of the global scour pit and can be determined using Eq. 2. The estimation of S_d depends largely on the depth of the global scour pit P and its upstream slope β , which can vary

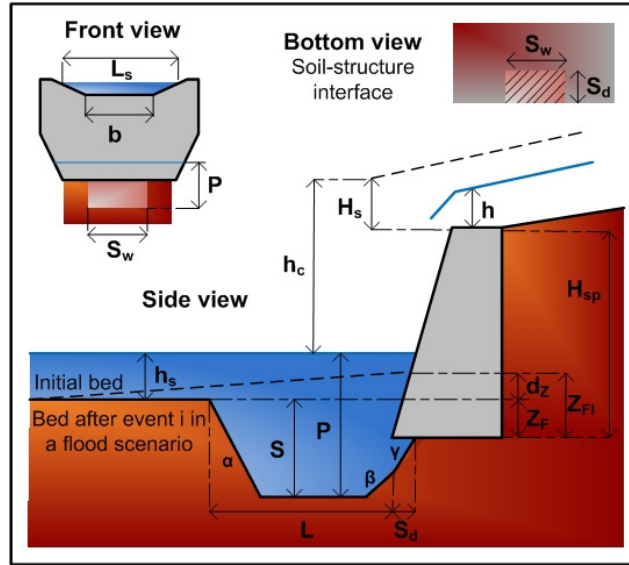


Figure 4: Key geometric and hydraulic parameters for estimating the dimensions of global and local scour pits.

338 based on soil characteristics. The global scour pit is modeled as a trapezoidal shape with side slopes of $\alpha = \beta = 1/1$
 339 (m/m), as determined from the non-dimensional scour pit profile obtained from the experimental study conducted by
 340 [50]. Additionally, the upstream side of the local scour is assumed to have a steeper slope of $\gamma = 2/1$ (m/m) compared
 341 to the upstream slope of the global scour pit. According to this assumption, the calculation of S_d is determined through
 342 simple geometric calculations (Chahrour et al., 2021). Figure 4 illustrates the geometry of the global and the local scour
 343 pits, along with the parameters used for estimating their dimensions.

3.2.2. Check Dam's Stability Justification

344 The formation of a local scour pit poses a risk to the stability of the check dam, as it reduces the soil bearing capacity
 345 and increases applied loads potentially leading to structural failure. The variables required for stability assessment are
 346 obtained when the global scour pit reaches its maximum depth, denoted as P_{max} , during each flood event. However,
 347 it should be noted that P_{max} can vary depending on the peak discharge of each event. In other words, the maximum
 348 depth of the scour pit for event $i + 1$ may be less than that of event i due to the refilling of the scour pit by transported
 349 materials. Nevertheless, in this study, it is assumed that the refilling of materials does not contribute to enhancing the
 350 structural stability. It is important to acknowledge that even if the scour pit appears to be filled, the materials may not
 351 be densely compacted as they were in the initial state. Consequently, the dimensions of the local scour pit, represented
 352 by S_d and S_w , which play a crucial role in the dam's stability, are assumed to consistently increase after each flood
 353 event. Specifically, if the values of S_d and S_w for event $i + 1$ are less than those of event i , the values corresponding
 354 to event $i + 1$ are adjusted to match those of event i .

355 The external stability justification for check dams, whether they are of the cantilever or gravity type, varies based
 356 on the applicable standards. In this study, the calculation principles and safety factors follow a French standard Groupe
 357 de travail (1993), which serves as a methodological example. To ensure the external stability of a check dam, it is
 358 necessary to verify the following three equilibrium conditions:
 359

360 *Stability against exceeding soil bearing capacity:* refers to the ability of the soil under the dam's base to withstand
 361 the vertical loads exerted on it. It is achieved by satisfying the following condition:

$$\sigma_{adm} > q'_{ref} \quad (6)$$

362 where σ_{adm} (KN/m^2) is the maximum admissible stress the soil can withstand without failure, while q'_{ref}
 363 (KN/m^2) represents the actual stress exerted on the soil. The estimation of σ_{adm} mainly depends on the

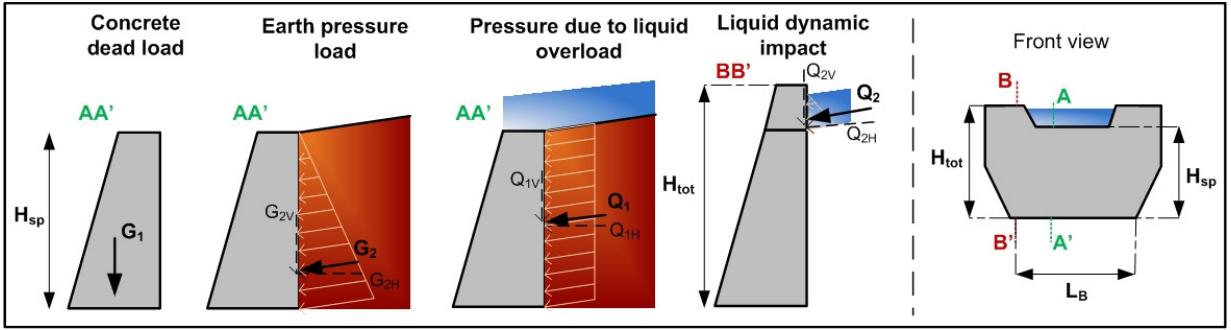


Figure 5: Permanent and variable loads acting on a concrete gravity dam.

properties of the soil. On the other hand, the estimation of q'_{ref} typically involves analyzing the normal stress distribution across the entire base of the dam. However, when local scouring occurs, soil removal specifically affects the central area under the dam's base. Consequently, the stress redistribution is limited to the remaining portions of soil in contact with the dam. This implies that the stresses are primarily transferred to the non-scoured soil. Therefore, the calculation of q'_{ref} is strongly influenced by the dimensions of the local scour pit S_d and S_w which vary after each event within a flood scenario.

Stability against overturning: refers to the ability of the dam to withstand the overturning moment M_O (KN.m) generated by the destabilizing loads. This requirement is fulfilled by ensuring the following condition is met:

$$M_S > M_O \quad (7)$$

where M_S (KN.m) is the stabilizing moment generated by the loads acting on the check dam and contributes to its stability. In case of local scouring, the stability against overturning is significantly impacted when the width of the scour pit S_w matches the length of the dam's base L_B . This occurs because the axis of rotation of the dam is shifted inward, resulting in a significant reduction in the stabilizing moment.

Stability against sliding: refers to resist the horizontal force R_H (KN) exerted on it. To prevent sliding, the following condition must be satisfied:

$$R_{SL} > R_H \quad (8)$$

where R_{SL} (KN) denotes the maximum frictional force that resists sliding at the interface between the soil and the dam structure. During local scouring, the value of R_{SL} is influenced since it depends on the compressed width of the dam's base.

This study focuses exclusively on concrete gravity dams. Figure 5 presents all the possible loads that act on this type of dam. These loads are of paramount importance in evaluating the three aforementioned conditions and ultimately justifying the external stability of the dam. It is worth noting that these conditions are assessed using a combination of loads multiplied by safety factors corresponding to the ultimate limit state (ULS) conditions.

Given the simulation of a flood scenario involving multiple flood events, the stability of the check dam will vary after each event. In order to assess the deterioration trajectory of the dam, it is essential to use an indicator that encompasses all potential causes of stability failure. While analyzing the overall stability level of a check dam, it is important to consider the combined effects of soil bearing capacity, overturning, and sliding failures. To address this, a global deterioration indicator, denoted as S_g , is proposed. This indicator normalizes and aggregates sub-indicators associated with the three failure mechanisms related to the external stability of the dam. S_g combines three sub-indicators: the bearing capacity stability ratio S_{BC} , the overturning stability ratio S_{OT} , and the sliding stability ratio

392 S_{SL} . These sub-indicators are normalized to fit within the interval [0, 1], where a value of 0 represents a total failure and
 393 a value of 1 corresponds to the maximum stability level. By using this normalization approach, the three sub-indicators
 394 can be compared and combined to provide a comprehensive assessment of the check dam's stability.

395 This study builds upon the global stability indicator introduced by Chahrour et al. (2021) for check dams by
 396 incorporating weighting factors for each sub-indicator. The non-dimensional global stability indicator is therefore
 397 defined by the following equation:

$$S_g = (\sqrt{S_{BC}^\alpha \cdot S_{OT}^\beta \cdot S_{SL}^\gamma})^{1/(\alpha+\beta+\gamma)} \quad (9)$$

398 where:

$$S_{BC} = \frac{\sigma_{adm} - q'_r e f}{\sigma_{adm}};$$

$$S_{OT} = \frac{M_S - M_O}{M_S};$$

$$S_{SL} = \frac{R_{SL} - R_H}{R_{SL}}$$

399 Recognizing the different levels of importance of the stability indicators S_{BC} , S_{OT} , and S_{SL} in determining the
 400 overall stability indicator S_g , weighting coefficients α , β , and γ are introduced. The selection of these weighting
 401 coefficients takes into account the influence of the scouring phenomenon on each stability indicator. These powers
 402 reflect the varying degrees of impact that scouring has on each indicator. Moreover, Eq. 9 indicates that the dam is
 403 considered to have completely failed if any of the sub-indicators reaches the failure threshold 0.

404 3.2.3. Check Dams' Dependency Analysis

405 To analyze the interdependencies between check dams implemented in series, it is essential to assess the influence
 406 of the presence or absence of one dam on the behavior of the other dams. In the case of a protection system with three
 407 identical check dams, D_1 , D_2 , and D_3 , four distinct modeling cases are considered:

408 *Case 1:* all three dams D_1 , D_2 , and D_3 exist in the system;

409 *Case 2:* absence of D_2 ;

410 *Case 3:* absence of D_3 ;

411 *Case 4:* absence of D_1 .

412 For each modeling case, comprehensive simulations are conducted, encompassing both the hydraulic aspects of
 413 the torrential flow and the stability of the check dams. This involves examining the dynamic deterioration of each dam
 414 within the specific case. Consequently, for each flood scenario, a total of nine simulations are performed, comprising
 415 three simulations for each dam (D_1 , D_2 , and D_3). The configurations of the torrential protection systems for each case
 416 are illustrated in fig. 6, providing a visual representation of the modeled scenarios.

417 3.3. Maintenance Decision-Making Model

418 The main objective of the developed approach is to support maintenance decision-making for multi-component
 419 protection systems. The check dam stability model allows us to identify the critical dams that could significantly
 420 impact the behavior of other dams in the event of their failure (absence). This initial stage helps prioritize maintenance
 421 actions by determining which dams within a protection system should be addressed first. In the subsequent stage,
 422 maintenance strategies for a specific dam may vary based on factors such as optimal inspection timing, choosing
 423 between waiting for more severe deterioration before repair or conducting early repairs, and determining the appropriate
 424 type of maintenance operations (minor, major, or corrective). For the managers of protection structures, the challenge
 425 is to select the most cost-effective solution while considering that longer intervals between maintenance increase the
 426 risk to downstream protected assets and people.

427 Stochastic Petri nets (SPNs) are a modeling technique used to analyze the behavior of systems over time, taking into
 428 account deterioration mechanisms and maintenance actions. An SPN model typically comprises four main elements:

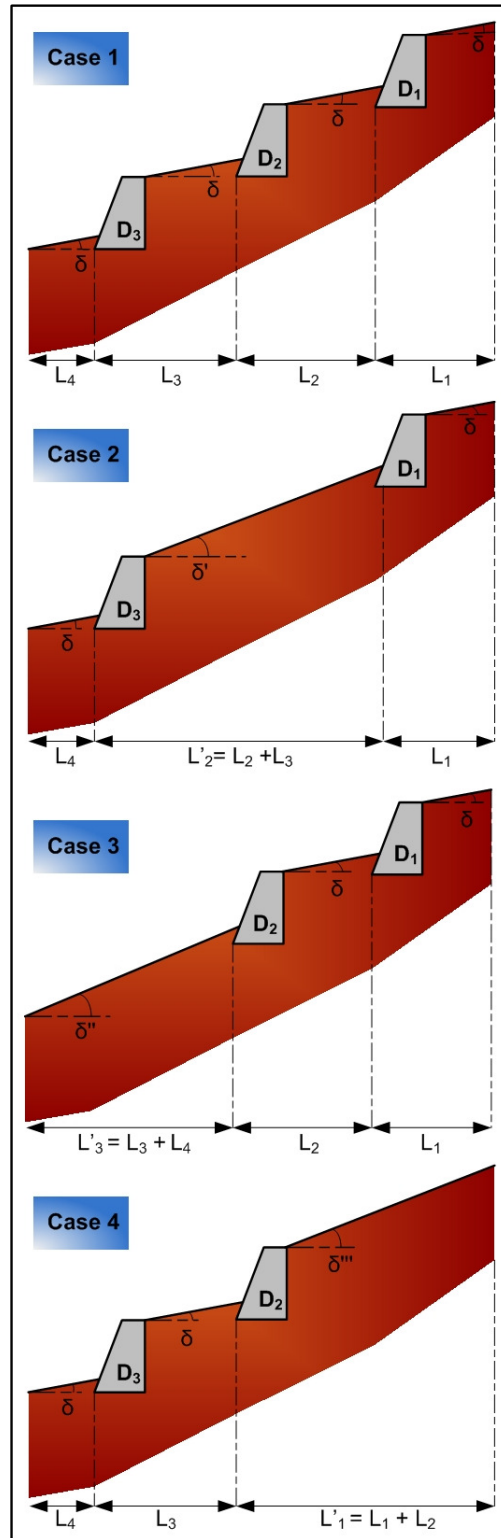


Figure 6: Four configurations of a protection system with three identical check dams corresponding to four modeling cases.

places, tokens, transitions, and arcs. A place within an SPN model is represented by a circle and can refer to a specific condition or required resource that must be satisfied or available before a particular action can be executed. A token, usually present in a place, is depicted as a small solid black circle and signifies the fulfillment of a specific condition or the availability of resources in the corresponding place within the SPN model. A transition is represented by a rectangle corresponds to events or actions that occur after a specified time. Transitions enable the movement of tokens between places in the SPN model. They can be associated with either a stochastic time law or a deterministic time value, determining when the transition takes place. An arc is represented by an arrow and connects a place to a transition, or vice versa. Each arc is associated with a multiplicity, which is a natural number indicating the number of tokens required or produced for the transition to occur. If the multiplicity is not explicitly shown above the arc, it is assumed to be equal to one by default.

It is worth mentioning that the SPN tool, while well-suited for addressing dynamic deterioration and maintenance processes in complex systems, is just one of several effective modeling techniques. Other options, such as colored Petri nets (CPNs) or stochastic activity networks (SANs), could have been considered as well. The decision to use SPN tools is not claimed to be the optimal selection but is verified to effectively achieve the study's intended objectives. The SPN model developed in this study to support maintenance decision-making for check dams consists of three distinct processes: deterioration process, inspection process, and maintenance process. Each of these processes is described in details in the following sections.

3.3.1. Stochastic Deterioration Process

The scenario-driven physics-based model developed in this study represents the physical process behind the deterioration of check dams over time. However, this model is not optimally adequate for the analysis and evaluation of different maintenance, given its sequential execution of multiple sub-models. To address this, we have developed a stochastic deterioration process using SPNs, which acts as a meta-model of the physics-based model. This enhanced model simplifies and encompasses the physical deterioration process, accounting for its variability and uncertainty comprehensively. Importantly, it offers the flexibility to easily implement different maintenance policies.

The deterioration process in the SPN model represents the evolution of a check dam's condition throughout its lifetime. The places within the model represent the different possible deterioration states that the dam can undergo. The transitions in this process are stochastic, meaning that they are associated with probability laws that determine the transition time between the dam's states. These transitions reflect the inherent uncertainty and variability in the deterioration process, allowing for a realistic representation of the dam's condition over time.

A check dam undergoes a progressive evolution from its initial state to various deteriorated states until it eventually reaches a completely failed state, resulting in its collapse. In order to track the deterioration trajectory of the check dam, the global stability indicator S_g is selected as the deterioration indicator. In this study, the dam is assumed to reside in four distinct states, each representing a specific condition related to the dam's stability. These states are defined as follows:

State 1: good condition with $S_2 < S_g \leq S_1$

State 2: poor condition with $S_3 < S_g \leq S_2$

State 3: very poor condition with $S_4 < S_g \leq S_3$

State 4: failed condition with $S_5 \leq S_g \leq S_4$

where $S_1, S_2, S_3, S_4,$ and S_5 are the global state indicator thresholds that define the intervals for the different states of the check dam. The threshold $S_1 = 1$ represents the initial new state of the dam, while $S_5 = 0$ corresponds to the collapse of the structure. The intermediate thresholds $S_2, S_3,$ and S_4 are determined through expert judgment and can be subject to discussion and modification as needed.

The transition times between these states are determined by learning the transition probability laws from the scenario-driven physics-based model, presented in section 3.2. This model generates multiple observations of check dam deterioration trajectories, with the number of observations depending on the considered flood scenarios. From these trajectories, realizations of random transition times between the defined states can be obtained (see fig. 7). The transition laws can finally be learned by estimating non-parametric cumulative distribution functions for each transition.

Figure 8a represents the deterioration process within the overall SPN model. Places P_1 - P_4 correspond to the four states of the check dam, representing the good, poor, very poor, and failed conditions, respectively. The model assumes that the dam is initially in a good condition, indicated by the presence of a token in P_1 at $t = 0$. Stochastic

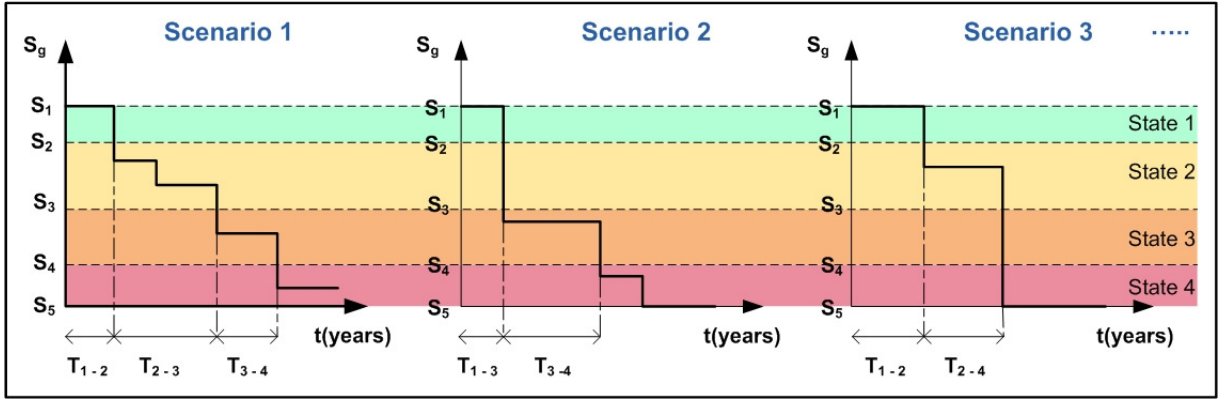


Figure 7: Example illustrating different deterioration trajectories and variations in transition times based on the modeled flood scenario.

transitions, denoted as T_{i-j} , govern the movement of the token between place i to place j , representing the evolution of the dam's condition over time. For instance, T_{2-3} connects states 2 and 3, while T_{2-4} connects states 2 and 4. The firing (occurrence) of stochastic transitions is determined by the firing delay time, which is drawn from probability distributions associated with each transition. In other words, once all the transition conditions are met, a transition is fired when its firing delay time is reached. Upon firing, the token moves from the input place of the transition to its output place.

The deterioration process of a dam is not necessarily gradual due to the stochastic nature of flood scenarios and the influence of the presence or absence of other dams. Depending on the specific scenario and dam configuration, the dam can move from one state to another through different pathways. For instance, in one case, the dam may degrade gradually through transitions T_{1-2} , T_{2-3} , and T_{3-4} , while in another case, it could degrade rapidly through T_{1-2} and T_{2-4} , or directly through T_{1-4} . This variation in deterioration trajectories and transitions occurs because each dam's behavior is influenced by the specific conditions and interactions within the multi-component protection system.

3.3.2. Periodic Inspection Process

Field inspections are generally conducted to assess the condition of check dams. During these visits, specific deterioration indicators are measured to determine the state of the dams and identify necessary maintenance operations. However, field inspections for check dams in mountainous regions pose unique challenges due to isolation, extreme weather, rough terrain, and limited annual budgets, often leading to varying inspection frequencies. In such regions, there are seasonal variations in rainfall, with high rainfall in summer and relatively low rainfall in autumn, which significantly impacts the probability of dam failures. Managers of check dams must choose the most appropriate inspection timing based on these seasonal variations. Various scenarios can be considered regarding inspection frequency such as immediate post-rainfall assessments and scheduled annual visits, with inspection schedules depending on factors like torrent activity and available resources. In this study, it is assumed that inspections are carried out annually, once per year.

Figure 8b represents the inspection process within the developed SPN model. Initially, a token resides in place P_5 , which is connected to the transition T_5 representing the periodic inspection. Subsequently, after a year has passed, the transition T_5 is fired, causing the token to move from P_5 to P_6 , where the inspection occurs. Depending on the condition of the inspected dam, one of the immediate transitions, namely T_6 , T_7 , or T_8 , will immediately fire, resulting in the appearance of a token in either P_7 , P_8 , or P_9 respectively. In order to schedule the next inspection, the transition T_4 also fires simultaneously, leading the token in P_6 to return to P_5 , where it awaits the next inspection after another year.

3.3.3. Condition-based Maintenance Process

Different maintenance operations can be carried out based on the condition of the dam to either restore it to its initial state or mitigate the level of deterioration. This aligns with the implementation of a condition-based maintenance policy (CBM) (Alaswad and Xiang, 2017), specifically designed for discrete deterioration processes. Several CBM policies

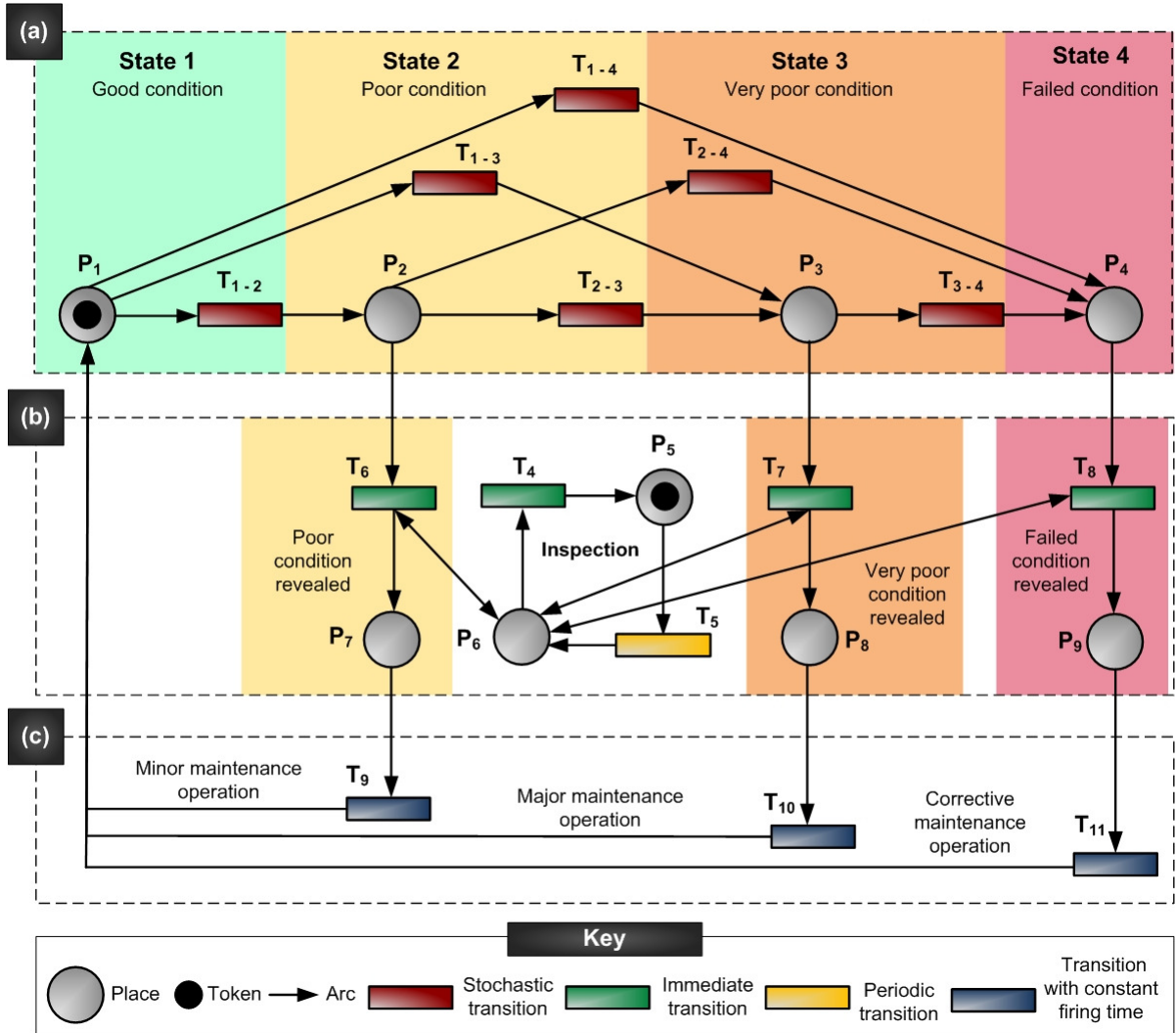


Figure 8: SPN model illustrating the different processes involved in modeling the stochastic behavior of a deteriorated and maintained check dam. (a) Deterioration process; (b) Inspection process; and (c) Maintenance process.

513 can be implemented for the deterioration process under consideration. The policy, illustrated in Figure 8c, has been
 514 adopted for this study. When the dam is in a good state, no maintenance operation is required. However, if the dam is
 515 detected to be in a poor, very poor, or failed state, indicated by the presence of a token in $P_7, P_8,$ or P_9 respectively,
 516 minor, major, or corrective maintenance operation is assigned. Minor maintenance operations, such as filling the scour
 517 fit with rock or concrete riprap, and major maintenance operations, such as anchoring or adding counterfort beams,
 518 are considered preventive measures applied to prevent the total failure of the dam. On the other hand, corrective
 519 maintenance operations are carried out when the dam reaches a failed state, requiring complete reconstruction. All
 520 these operations are classified as perfect maintenance operations, which aim to restore the system to its initial new
 521 state once they are completed. This concept is emphasized in the SPN model as follows: when transition $T_9, T_{10},$ or
 522 T_{11} is fired, a minor, major, or corrective operation is performed respectively, and the token in $P_2, P_3,$ or P_4
 523 returns to P_1 . The firing delay times associated with Transitions $T_9, T_{10},$ and T_{11} represent the time required to schedule and
 524 carry out the repair work.

525 It should be emphasized that the dam has the potential to deteriorate from one state to another prior to the planned
 526 inspection. This means that the dam may not be repaired immediately upon reaching a state that requires maintenance.
 527 For instance, if the dam is in state 2, there are three possible scenarios:

1. If transition T_6 fires first, indicating that the inspection has taken place, the token in P_2 moves to P_7 waiting for a minor maintenance operation to be performed. 528
2. If transition T_{2-3} fires first, the token in P_2 moves to P_3 , indicating that the dam has deteriorated to state 3 before any maintenance was conducted. This could be due to factors such as a subsequent flood event that caused further deterioration of the dam within a short period of time. 529
3. If transition T_{2-4} fires first, the token in P_2 moves to P_4 , indicating that the dam has deteriorated directly to state 4 before undergoing any inspection. This could be a result of a severe flood event that rapidly caused significant deterioration of the dam. 530

These possibilities highlight the potential for the dam's condition to worsen before necessary maintenance actions are undertaken, illustrating the dynamic nature of the deterioration process. In this study, an important assumption is made regarding the number of maintenance operations that can be conducted before a corrective maintenance operation. Specifically, it is assumed that only three minor maintenance operations and two major maintenance operations can be executed on a single check dam. Once these limits are reached, further minor and major maintenance operations are prohibited. However, the completion of a corrective maintenance operation will reset the restrictions, allowing for the resumption of minor and major operations. This assumption is considered to better reflect real-world conditions, recognizing that the effectiveness of minor and major operations in improving the dam's condition and reducing its deterioration level may reach a limit over time. 531

The flexibility of SPNs offers a significant advantage, as it makes it possible to use a consistent model structure, as shown in fig. 8, while accommodating different functionalities for the purpose of comparing various maintenance strategies. In this study, four maintenance strategies have been proposed: 532

Strategy 1: All maintenance operations are permitted. The dam is repaired when it reaches states 2, 3, or 4. 533

Strategy 2: Minor maintenance operations are prevented. The dam is allowed to deteriorate beyond state 2 without any maintenance intervention. 534

Strategy 3: Major maintenance operations are prevented. Once the dam reaches state 3, further deterioration to state 4 is permitted without any major maintenance. 535

Strategy 4: Only corrective maintenance operations are permitted. The dam is exclusively repaired when it reaches a completely failed state. 536

In order to compare the proposed maintenance strategies, each strategy is simulated separately in order to model the evolution of the maintained dam. Generally, for SPNs, the principle of Monte-Carlo simulation is used. Once the SPN model is constructed and the simulation period is identified, Monte-Carlo simulation starts and the tokens keep on moving around the model until t_f is reached. Applying this kind of simulation and repeating the draw of a random value several times, provide statistical estimates of specific quantities of interest. For each proposed maintenance strategy, two outputs are provided. Firstly, the average time spent by the dam in each defined state is calculated. This provides insights into the duration the dam remains in different conditions under each strategy. Secondly, the average number of maintenance operations performed over the specified simulation period is determined. This information helps evaluate the total cost of each strategy, given the cost of each maintenance operation. These outputs make it possible to compare the proposed maintenance in terms of cost, as well as the maximum availability of the dam, which refers to the duration it remains in a non-failed state. Ultimately, these results support risk managers in making informed decisions regarding cost-effective maintenance strategies. 537

4. Case Study: Modeling & Analysis of the Faucon Protection System 538

In this section, we provide a concise overview of the selected case study for this research. We begin by introducing the Faucon torrent and its protective system in France. The data required for conducting simulations in the sub-models discussed in Section 3 are presented. We specifically focus on the modeling of three consecutive check dams within the Faucon protection system. Additionally, we present and analyze the results obtained from the modeling of these dams over a period of 100 years. 539

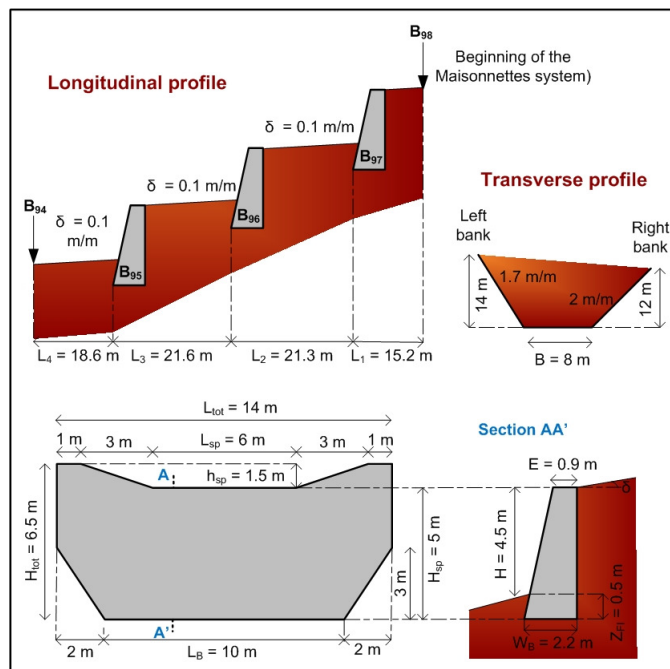


Figure 9: Key data for about the Faucon torrent and the check dams of the Broche System under study.

4.1. Faucon System: Description & Input Data

The Faucon torrent (see fig. 1b), located in the Alpes-de-Haute-Provence department of France, poses a significant threat of torrential floods to the Commune of Faucon de Barcelonnette. Extensive correction protection measures have been implemented on the torrent since the late 19th century, with a focus on mitigating torrential flood events. The torrent spans a length of 6.4 km and covers an area of 7.8 km², characterized by a steep slope and high solid transport. The channel's vulnerability to scouring phenomena is amplified by the presence of steep and easily erodible bed and banks. The Faucon torrent comprises seven protection systems, including five in the main flow channel (Broche, Maisonnettes, Granges Hautes, Les Clots, Rasinière) and two on tributaries (Champerousse, Affluent RG). Detailed data on the torrent, structures, maintenance activities, and associated costs can be found in the reference provided by ONF-RTM (2014).

A total of 81 check dams were constructed within the Faucon system between 1960 and 2014. This brings the overall count of structures built between 1865 and 2014 to at least 160. The construction cost for these 81 dams amounted to 5,583,000. Notably, the Broche system accounted for approximately 52% of the total expenditure. Maintenance expenses for these structures amounted to 677,000 €, with the Broche system representing the majority of the costs due to its extensive number of maintained structures. This study focuses on the Broche system, which is situated downstream of the Faucon torrent. This system holds significant importance, as it comprises a total of 24 dams that play a crucial role in mitigating torrential risks and protecting vulnerable assets and people located in the alluvial fan of the Faucon. Nevertheless, the location of these dams exposes them to significant erosion risks, necessitating careful assessment and maintenance considerations.

In this study, we aim to model and analyze three consecutive check dams located upstream in the Broche system. The purpose is to investigate the interdependence between these dams and provide insights for their maintenance decision-making. The dams, namely B₉₇, B₉₆, and B₉₅, are identical concrete gravity dams. Figure 9 provides the dimensions of these dams and their configuration along the longitudinal profile of the system, including the bed slope and distance between the dams. Additionally, the figure presents a cross-section of the Broche system at the location of these dams.

Geotechnical data concerning soil properties of the bed erodible layer, as well as the flow characteristics and volumetric weight of the dams, are provided in Table 1. A set of 100 flood event scenarios are generated for analysis, focusing specifically on clear water flood events with a ten-year return period. The peak discharges for each event

Table 1

Data used in this study: D_{30} , D_{50} , and D_{90} are the grain size distribution; Φ is the angle of friction; c is soil cohesion; ple is soil equivalent limit pressure; Ka is the earth pressure coefficient; γ_S , γ_C , and γ_L are respectively the volumetric weight of soil, concrete and liquid; DI is the dynamic impact factor of the flow.

D_{30} (m)	D_{50} (m)	D_{90} (m)	Φ (°)	c (KN/m ²)	ple (KN/m ²)	Ka -	γ_S (KN/m ³)	γ_C (KN/m ³)	γ_L (KN/m ³)	DI -
0.026	0.037	0.09	35	0	2000	0.27	18	24	10	5

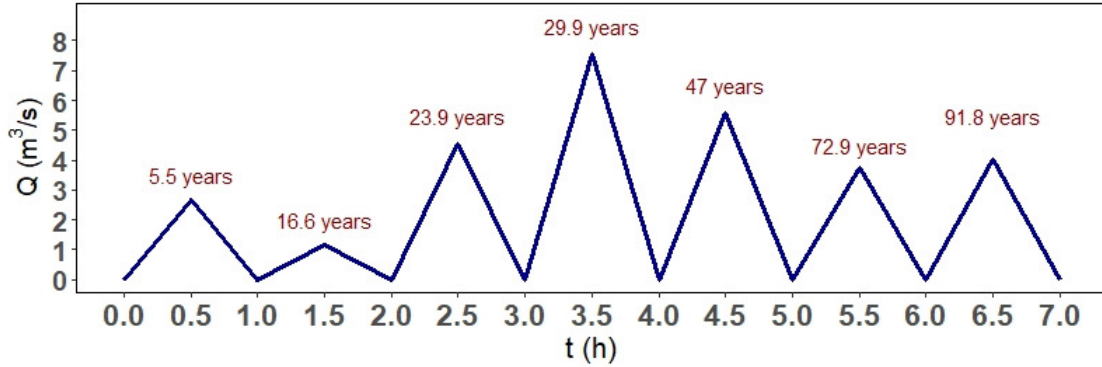


Figure 10: Hydrograph representing all events involved in one of the generated scenario over a period of 100 years. Each event is represented by its respective hydrograph, and the time of occurrence is indicated above each hydrograph.

within a scenario are randomly generated using a truncated gamma distribution. The average peak discharge is set $Q_{avg} = 6 \text{ m}^3/\text{s}$ with a shape parameter of 3 and a scale parameter of 2, while the maximum peak discharge is set $Q_{max} = 8 \text{ m}^3/\text{s}$. The hydrographs of the events are assumed to have a triangular shape, with a peak time $t_{peak} = 0.5$ hours and an end time $t_{end} = 1$ hour. The occurrence dates of the events in each scenario are generated using a Poisson distribution with a parameter $\lambda = \frac{1}{\text{return period}} = \frac{1}{10}$. These flood scenarios span a period of 100 years, and each scenario may contain a different number of flood events. Figure 10 shows the complete set of flood events within one of the generated scenarios.

All data mentioned above is used for performing torrential hydraulic modeling and check dam stability modeling. For the SPN model, which is developed for maintenance decision-making and implemented and evaluated using GRIF-Workshop developed by TOTAL and SATODEV (GRIF, 2021), the key input data required for simulation are the transition times. As mentioned before, the probability distributions governing the stochastic transitions in the deterioration process will be derived from the physics-based hydraulic and stability model. The deterministic transitions involved in the inspection and maintenance processes are provided in Table 2. T_5 corresponds to the inspection frequency; T_4 , T_6 , T_7 , and T_8 are the immediate transitions that governs the inspection process; and T_9 , T_{10} , and T_{11} represent the time needed to carry out the minor, major, and the corrective maintenance operations respectively.

The construction costs and maintenance costs for each dam in the Broche system are documented in ONF-RTM (2014). The average cost of construction for the three dams under study, namely B_{97} , B_{96} , and B_{95} , is used as the cost of a corrective maintenance operation, set at 174,000 €. By considering the provided information on the costs of various maintenance operations, the estimated costs for minor and major operations are 7,000 € and 50,000 €, respectively. These cost values are used to calculate the total cost associated with each maintenance strategy defined in Section 3.3.3, based on the number of operations performed within each strategy.

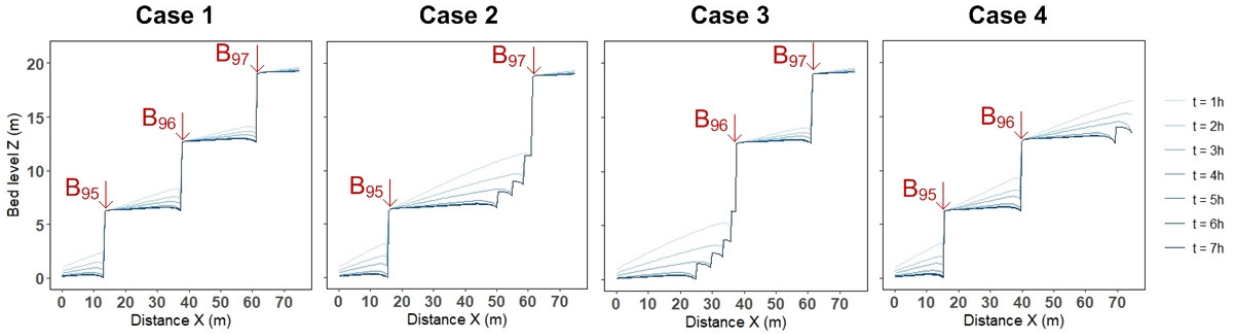
4.2. Model Implementation, Results, and Analysis

The torrential hydraulic modeling is conducted using LOGICCHAR, in which 100 simulations corresponding to the 100 generated flood scenarios are performed. The primary output of each simulation, which is crucial for calculating scouring, is the evolution of the torrent bed. Figure 11 shows the bed evolution of the torrent after simulating one of

Table 2

Transition times involved in the inspection and maintenance processes of the SPN model.

Process	Transition	Time (years)
Inspection	T_5	1
	$T_4 T_6 T_7 T_8$	0
Maintenance	T_9	0.0138
	T_{10}	0.083
	T_{11}	0.333


Figure 11: Bed level variation for different dam configurations after experiencing the flood events in one of the generated scenario.

626 the scenarios, which involves seven flood events occurring over 100 years. The figure illustrates the variation in the
 627 bed level across the longitudinal profile of the modeled section of the Broche system in the Faucon torrent over time
 628 after each of the seven flood events. It considers the different dam configurations presented previously in Section 3.2.3
 629 and visually represented in fig. 6.

630 The observed variations in the bed level provide valuable insights into the impact of flood events on the torrent
 631 bed and the effectiveness of different dam configurations in mitigating potential risks. Notably, in Case 1 where all
 632 three dams are present, the erosion downstream of each dam is relatively limited compared to other cases. In Case 2,
 633 where B_{96} is absent, excessive erosion is observed downstream of the upstream dam B_{97} . The zigzag shape of the bed
 634 indicates that the erosion depth has reached the maximum allowable depth of the erodible layer, which has been set
 635 at 5 m. Similarly, in Case 3, with the absence of B_{95} , the erosion downstream of the upstream dam B_{96} reaches the
 636 maximum depth of the erodible layer. In Case 4, where the dam B_{97} is absent, the most significant erosion occurs in
 637 the upstream area where there is no dam present. These findings highlight the dependency of an upstream dam on the
 638 presence of a downstream dam, as the absence of a downstream dam negatively affects the erosion downstream of its
 639 upstream dam (B_{97} depends on B_{96} , and B_{96} depends on B_{95}). This is due to the fact that the absence of a dam disrupts
 640 a fixed point in the longitudinal profile, leading to enhanced erosion upstream. The same results are observed across
 641 all the simulated scenarios.

642 The outputs generated by LOGICCHAR provide valuable information for conducting stability modeling of each
 643 dam. After each flood event in a scenario, the dimensions of local scouring, S_w and S_d , are estimated. Subsequently,
 644 the levels of sub-stability indicators S_{BC} , S_{OT} , and S_{SL} , are determined. The global stability indicator S_g is then
 645 calculated using Eq. 9, with weighting coefficients α , β , and γ set to 1.5, 1, and 0.5, respectively. These specific
 646 weighting coefficients were chosen for this study to primarily focus on analyzing the behavior of the dam when exposed
 647 to local scouring. In such cases, the dam's stability is likely to be at risk due to factors such as exceeding soil bearing
 648 capacity. Therefore, the sub-stability indicator S_{BC} is assigned the highest weighting coefficient. On the other hand,
 649 the dam's stability may also be significantly affected by overturning caused by scouring, especially when the width of
 650 local scouring S_w matches the length of the dam's base L_B . The occurrence of sliding is comparatively less likely than
 651 overturning and bearing capacity issues.

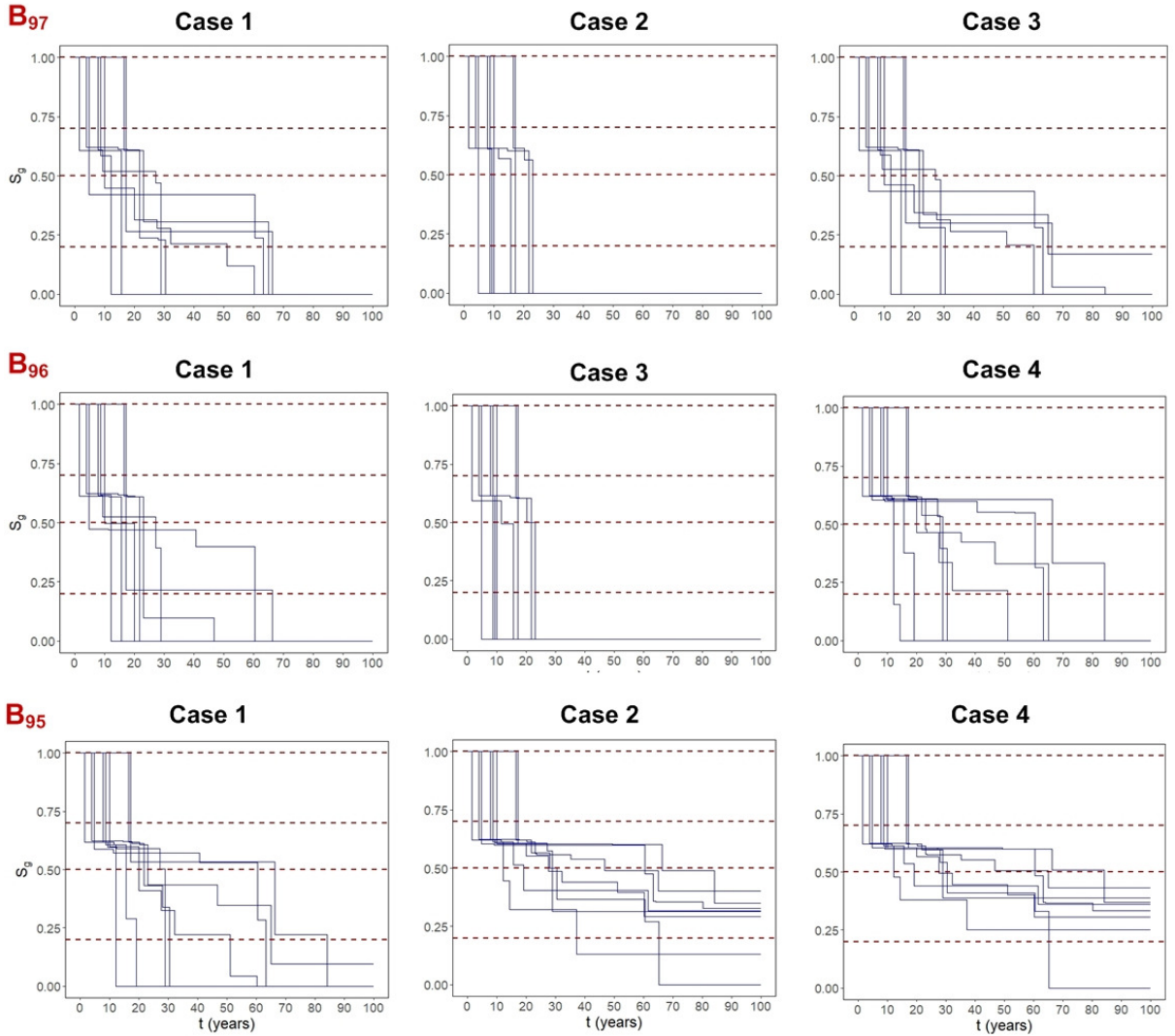


Figure 12: Deterioration trajectories of the dams under different configurations for ten flood scenarios. Blue curve: Evolution of the global state indicator S_g over time; red dashed lines: indicator thresholds.

The evolution of both scouring and stability indicators are tracked over a period of 100 years. The deterioration trajectories of the dam, represented by the global stability indicator (S_g) provide insights into the long-term efficacy of the dams. Figure 12. illustrates ten distinct trajectories for each dam in different configurations, represented by the considered cases. Each trajectory corresponds to one of the 100 generated scenarios, demonstrating the wide range of outcomes in dam performance. Regardless of the dependencies between the dams, the deterioration rate of each dam is influenced by the intensity (discharge) of the flood events in each scenario. The deterioration process is gradual when the scenario includes moderate flood events, while it becomes more rapid when high-intensity flood events occur early in the scenario. This highlights the importance of stochastic modeling to incorporate the potential variability in dam behavior during the analysis. Moreover, the figure clearly demonstrates the interdependencies among the dams, revealing that the absence of a downstream dam results in an increased deterioration rate for each individual dam. For instance, in Case 2 where dam B_{96} is absent, the deterioration of dam B_{97} (upstream of B_{96}) occurs at a faster rate compared to Case 1 where B_{96} is present. Similarly, in Case 3, the deterioration rate of dam B_{96} is higher than in Case 1 due to the absence of dam B_{95} downstream of B_{96} . On the contrary, the absence of an upstream dam appears to have a positive impact on the downstream dam's deterioration rate. For instance, in Case 2 where B_{96} is missing, the

Table 3

Number of observations attained by each transition for each dam and in each configuration.

Configuration	Case 1			Case 2		Case 3		Case 4	
Dam	B_{97}	B_{96}	B_{95}	B_{97}	B_{95}	B_{97}	B_{96}	B_{96}	B_{95}
T_{1-2}	81	86	98	48	99	83	46	100	100
T_{1-3}	15	10	2	16	0	15	4	0	0
T_{1-4}	4	4	0	36	1	2	50	0	0
T_{2-3}	51	45	66	19	78	55	13	73	82
T_{2-4}	30	41	30	29	12	27	32	25	4
T_{3-4}	50	50	51	34	25	50	18	56	26

Table 4

Parameters of the log normal distributions corresponding to transitions with low number of attained observations. μ : log mean; σ : log standard deviation.

Configuration	Case 1			Case 2	Case 3		Case 4		
Dam	B_{97}	B_{96}		B_{95}	B_{95}	B_{97}	B_{96}		B_{95}
Transition	T_{1-4}	T_{1-3}	T_{1-4}	T_{1-3}	T_{2-4}	T_{1-4}	T_{1-3}	T_{2-3}	T_{2-4}
μ	1.12	2.09	1.12	1.86	3.66	1.86	2.53	1.55	3.6
σ	1.32	0.6	1.32	0.08	0.68	0.08	0.72	1.43	0.42

deterioration rate of B_{95} is lower compared to Case 1, where the upstream dam B_{96} is present. Similarly, in Case 4 where B_{97} is absent, the deterioration rate of B_{96} is lower than in Case 1 where B_{97} is present. This can be attributed to the fact that in the absence of an upstream dam, erosion primarily occurs in the upstream areas where there is no fixed point in the longitudinal profile. Furthermore, most of the eroded materials from the upstream tend to deposit downstream, thereby enhancing the stability of the downstream dam through additional support. However, it is important to note that these results only pertain to a limited section of the longitudinal profile and do not consider the entire protection system. Hence, the absence of an upstream dam should not be regarded as entirely positive, as it neglects the potential support it provides to other upstream dams within the Broche system, which are not considered in this study.

To calculate the transition times between the states of the dams, it is necessary to define thresholds for each state indicating different conditions. In this study, the thresholds for the states, which represent good, poor, very poor, and failed conditions, are defined as $S_1 = 1$, $S_2 = 0.7$, $S_3 = 0.5$, $S_4 = 0.2$, and $S_5 = 0$.

The analysis of the deterioration trajectories of the dams has revealed that certain transitions have a limited number of observations or are completely absent in some cases. For instance, in Case 3, dam B_{96} has a low number of observations (only 4 out of 100 scenarios) for transition T_{1-3} , while in Case 4, dam B_{95} lacks transitions T_{1-3} and T_{1-4} across all 100 scenarios. The number of observations attained by each transition for each dam and in each configuration id given in Table 3. Given the limited data sets, transitions with fewer than 15 values are assumed to follow a log-normal distribution with specified log mean μ and log standard deviation σ , as provided in Table 4. Transitions with no observations (i.e., 0 values) are excluded from the deterioration process of the Stochastic Petri net model presented in fig. 8. For transitions with a sufficient number of observations (data sets exceeding 15 values), an empirical cumulative distribution function (CDF) is estimated using the Kaplan-Meier estimator (Kaplan and Meier, 1958) and presented in fig. 13 as the transition laws. Furthermore, it should be noted that in some scenarios, a dam reaches a specific state i and does not progress to a more deteriorated state j within the duration of the simulation (100 years). In such cases, there is no transition between states i and j . However, this information indicates that the dam ceases to deteriorate after reaching state i . These censored information are considered when estimating the cumulative distribution functions (CDFs). In the cases where censored information are present, the probability of transitioning from state i to state j does not reach a value of 1, as clearly shown in fig. 13.

The obtained probability laws for all stochastic transitions involved in the deterioration process serve as inputs to the SPN model. Each transition originating from the same state (place) is assigned a firing probability based on the number of observations it has attained. For instance, in Case 1, for dam B_{97} , the number of observations for transitions

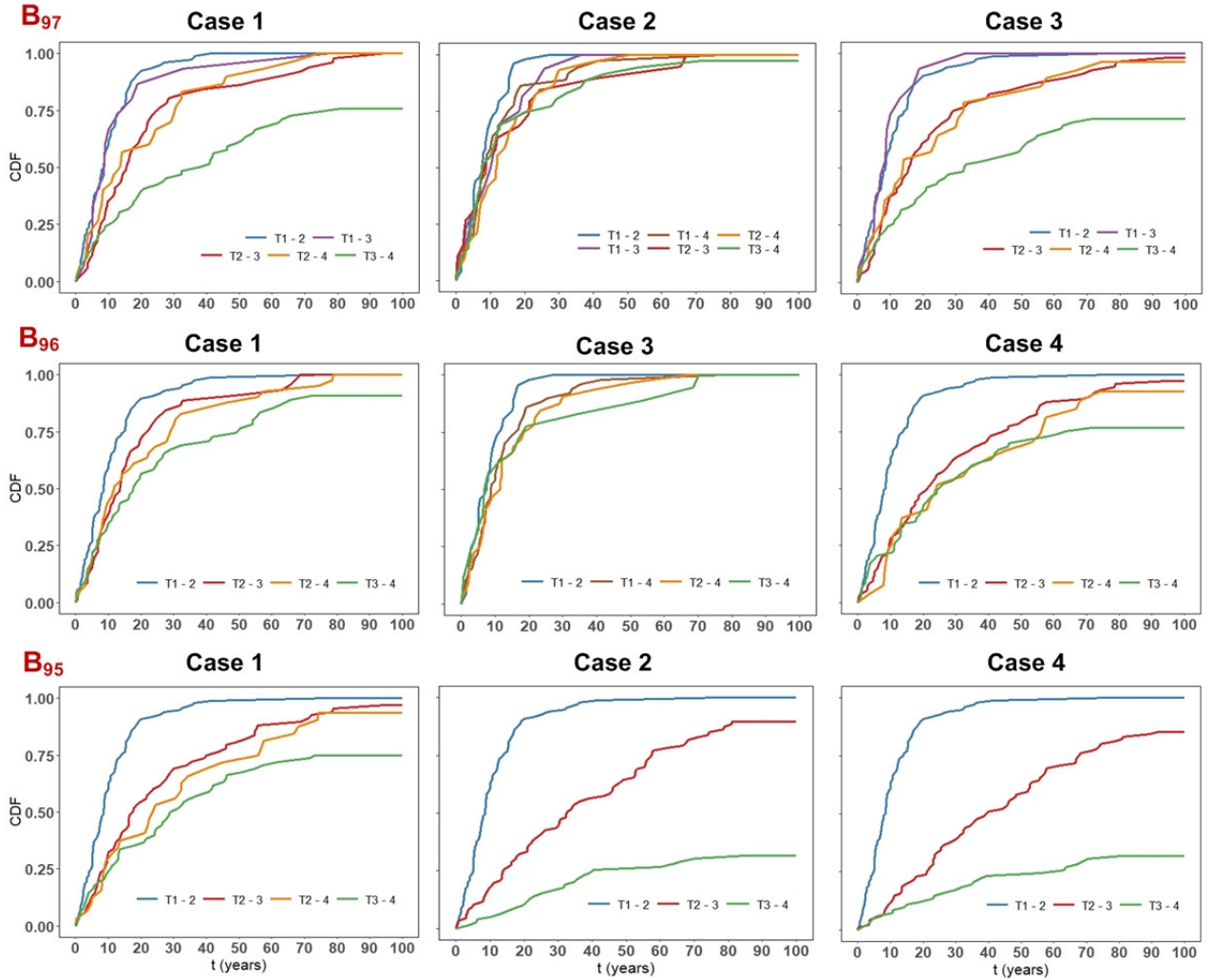


Figure 13: Cumulative distribution functions of stochastic transitions in the deterioration process of the SPN model, for each dam under the different configurations.

T_{1-2} , T_{1-3} , and T_{1-4} originating from place P_1 are 81, 15, and 4, respectively. Therefore, the firing probabilities for these transitions are 0.81, 0.15, and 0.04, respectively.

Given the stochastic nature of the SPN model, the sufficiency of simulations is determined by the point at which the results stabilize and converge, indicating a consistent outcome. In our study, we conducted a total of 1000 Monte-Carlo simulations, and it's worth noting that for all the implemented maintenance strategies, convergence was achieved after 500 simulations. Additionally, it's important to highlight that simulations using the SPN model are efficient in terms of duration, typically requiring only a few minutes to complete 1000 simulations. As previously mentioned, Monte-Carlo simulations of the developed SPN model provide statistics on the mean sojourn time of the dam in each defined state and the number of minor, major, and corrective operations performed over 100 years. The outcomes obtained for each maintenance strategy are summarized in Tables 5 and 6, respectively. The results in these tables offer valuable insights into the long-term performance and maintenance requirements of the interdependent system of check dams.

Table 5 shed light on the varying effects of different maintenance strategies on the longevity and condition of the dams in different configurations. A noticeable trend is observed among the strategies: in strategies 1 and 3, the dams across all configurations spend a longer duration in state 1 compared to strategies 2 and 4. This can be attributed to the fact that strategies 1 and 3 prioritize early maintenance with minor operations as soon as the dams show signs of deterioration. On the other hand, strategies 2 and 4, which restrict minor maintenance, result in longer duration in state

Table 5

Mean sojourn time (in years) spent by each dam in the four defined states depending on the adopted maintenance strategy.

Configuration		Case 1			Case 2		Case 3		Case 4	
Dam		B_{97}	B_{96}	B_{95}	B_{97}	B_{95}	B_{97}	B_{96}	B_{96}	B_{95}
Strategy 1	State 1	69.05	69.45	59.53	89.72	56	67.15	91.56	57.30	50.90
	State 2	25.41	26.43	38.59	5.66	42.65	26.02	2.98	41.08	48.15
	State 3	4.64	2.98	1.42	1.6	1.06	6.16	1.19	1.23	0.78
	State 4	0.77	1.03	0.38	2.9	0.22	0.55	4.17	0.31	0.11
Strategy 2	State 1	37.63	37.55	30.29	59.25	27.63	35.63	66.53	28.14	23.06
	State 2	55.54	56.09	65.17	35.45	68.63	55.68	28.07	68.21	74.92
	State 3	5.56	4.64	3.75	2.04	3.29	7.65	0.71	3.02	1.8
	State 4	1.12	1.58	0.67	3.12	0.32	0.88	4.61	0.52	0.11
Strategy 3	State 1	53.31	61.35	55.82	75.45	47.41	53.76	78.35	45.5	44.12
	State 2	13.08	15.57	26.42	3.33	30.58	12.81	2.41	29.11	34.92
	State 3	32.44	21.77	17.16	17.88	21.78	32.46	15.01	15.79	20.82
	State 4	1.17	1.31	0.6	3.33	0.24	0.97	4.23	0.6	0.14
Strategy 4	State 1	23.96	28.54	21.95	48.51	14.09	23.73	57.37	19.85	12.15
	State 2	35.92	40.24	46.44	28.75	41.33	36.61	24.63	49.3	48.74
	State 3	38.73	29.29	30.57	19.18	44.21	38.39	13.35	29.86	38.81
	State 4	1.39	1.93	1.04	3.56	0.37	1.28	4.65	0.99	0.29

Table 6

Average number of maintenance operations applied to each dam depending on the adopted maintenance strategy.

Configuration		Case 1			Case 2		Case 3		Case 4	
Dam		B_{97}	B_{96}	B_{95}	B_{97}	B_{95}	B_{97}	B_{96}	B_{96}	B_{95}
Strategy 1	Minor	4.16	4.68	3.79	3.82	3.61	3.86	3.22	3.62	3.31
	Major	1.49	1.34	0.94	1.51	0.84	1.48	1.15	0.91	0.13
	Corrective	0.83	1.11	0.45	3.5	0.27	0.68	4.92	0.37	0.13
Strategy 2	Minor	0	0	0	0	0	0	0	0	0
	Major	1.88	1.63	1.39	1.72	1.45	1.79	1.01	1.4	1.28
	Corrective	1.3	1.84	0.8	3.67	0.37	1.04	5.39	0.61	0.15
Strategy 3	Minor	3.71	4.45	4.03	3.15	3.5	3.63	2.83	4.11	3.26
	Major	0	0	0	0	0	0	0	0	0
	Corrective	1.29	1.47	0.72	3.94	0.27	1.15	5	0.71	1.17
Strategy 4	Minor	0	0	0	0	0	0	0	0	0
	Major	0	0	0	0	0	0	0	0	0
	Corrective	1.63	2.27	1.28	4.22	0.44	1.54	5.47	1.17	0.35

711 2 (poor condition) for the dams. In strategies 3 and 4, where major maintenance is inhibited, the dams remain in state
 712 3 (very poor condition) for an extended period compared to strategies 1 and 2, where major operations are allowed.
 713 Notably, in strategy 4, where only corrective operations are permitted, the dams spend more time in deteriorated states
 714 2 and 3 compared to other strategies. This is due to the absence of preventive maintenance, leading to continuous
 715 deterioration until complete failure, necessitating their replacement with new structures.

716 Furthermore, Table 5 also highlights the impact of the absence or presence of a downstream dam on the behavior
 717 of the upstream dam. In case where maintenance operations are carried out, the upstream dam spends a longer duration
 718 in state 4, indicating a rapid deterioration leading to complete failure. However, the upstream dam tends to spend more
 719 time in state 1 due to the increased number of corrective maintenance operations conducted over the period of 100
 720 years, as indicated in Table 6. For example, in Case 1 where B_{96} is present, B_{97} resides in state 1 for approximately 69
 721 years. However, in Case 2 where B_{96} is absent, B_{97} resides in state 1 for almost 90 years, due to the larger number of

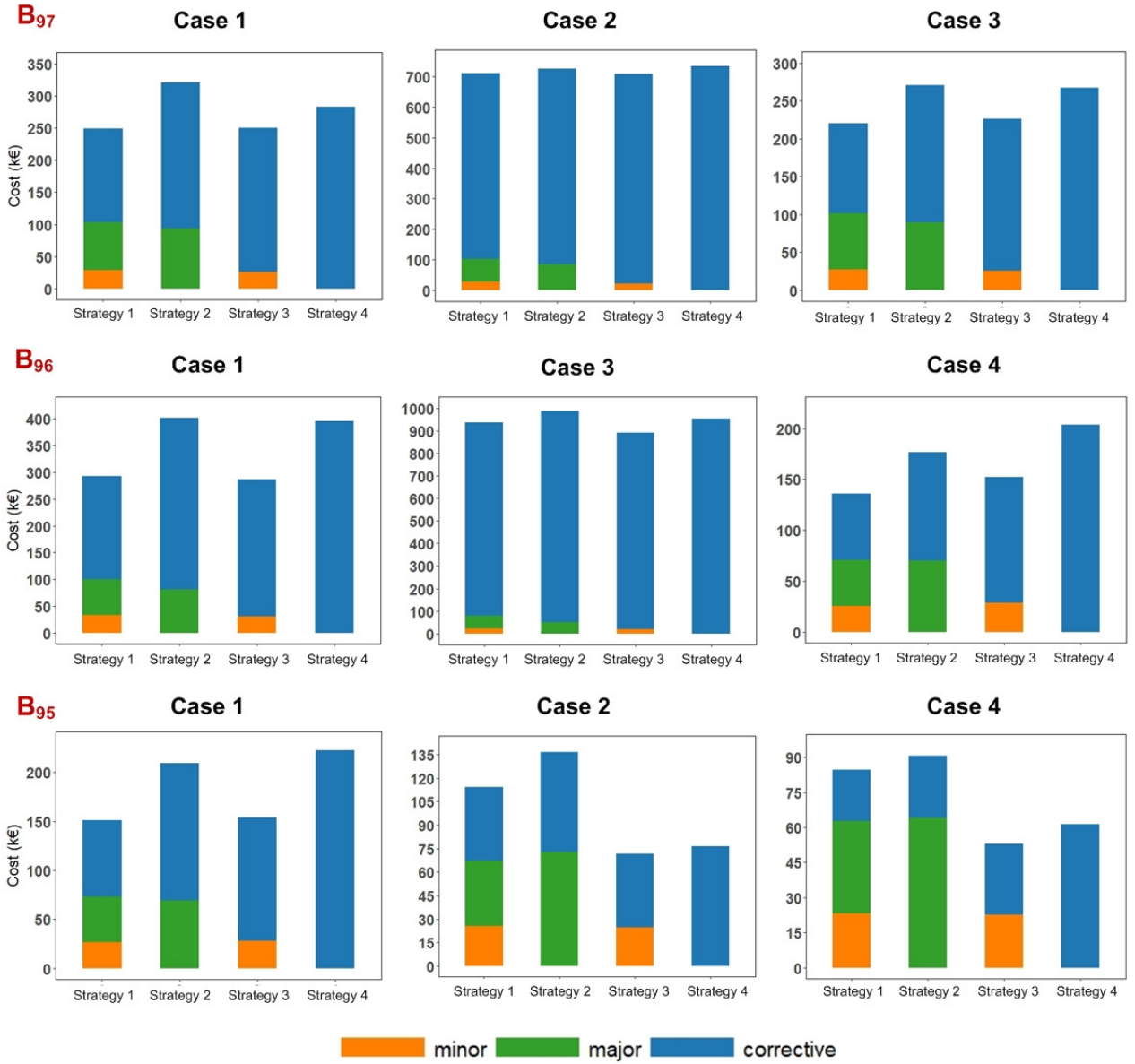


Figure 14: Average total cost of each maintenance strategy, for each dam under the different configurations.

corrective maintenance operations (approximately 4 operations). Similar results can be observed for B_{96} in the absence or presence of the downstream dam B_{95} .

Based on the obtained results regarding the deterioration trajectories, it is evident that when all dams are present (Case 1), dam B_{96} experiences a higher rate of deterioration compared to B_{97} and B_{95} , and both B_{97} and B_{96} deteriorate much faster than B_{95} . Therefore, prioritizing maintenance, the order of preference would be as follows: dam B_{96} is given the highest priority, followed by B_{97} , and finally B_{95} . In terms of prioritizing the maintenance strategies for each dam, the total expected cost of each strategy can be computed based on the statistics of the applied maintenance operations (as shown in Table 6). This enables a straightforward comparison and selection of the most cost-effective maintenance strategy. Figure 14 presents the total costs of the maintenance strategies, facilitating the sorting process to determine the optimal strategy.

The results presented in fig. 14 reveals that the most cost-effective maintenance strategy varies depending on the dam and the configuration in which it is implemented. In the presence of a downstream dam, strategies 1 and 3 prove to be less expensive compared to strategies 2 and 4 (e.g., B_{97} , B_{96} , and B_{95} in Case 1). This is due to the fact that these strategies prevent the dams from deteriorating to states that require costly maintenance operations. Instead, they are directly repaired through minor operations, which are considerably less expensive than major and corrective operations. In cases where the downstream dam is absent, all strategies exhibit similar costs for the upstream dam, as corrective operations dominate across all strategies (e.g., B_{97} in Case 2 and B_{96} in Case 3). In the absence of the upstream dam B_{97} (Case 4), strategy 1 is the most cost-effective for B_{96} , while strategy 3 proves to be the most cost-effective for B_{95} . Furthermore, in the majority of cases, maintenance strategy 2 attains the highest costs. This is because maintenance is applied only when the dam reaches critical states (states 3 and 4), necessitating expensive operations.

In conclusion, the absence of a downstream dam (e.g., B_{96} in Case 2 and B_{95} in Case 3) leads to increased maintenance costs regardless of the adopted maintenance strategy, compared to Cases 1 and 4. Conversely, the absence of the upstream dam B_{97} (Case 4) results in decreased maintenance costs compared to Case 1, where all dams are present. However, it is important to note that this does not imply that the configuration of dams in Case 4 is superior to that in Case 1, as we have not considered the entire reach of the Broche system. In reality, there are likely dams implemented upstream of dam B_{97} , necessitating the presence of dam B_{97} . Therefore, if we consider the studied reach as representative of the entire flow channel of the torrent, the configuration of dams in Case 4 would be optimal. However, in the actual case study, the already implemented configuration of Case 1 proves to be optimal as it attains lower maintenance costs compared to Cases 2 and 3.

5. Conclusion

In this study, a scenario-driven deterioration model is developed to model the behavior of interdependent system of check dams over time. A decision-aiding model is also developed to support maintenance decision-making of check dams using stochastic Petri nets (SPNs). The analysis considered different configurations of dams and examined the impact of various maintenance strategies on the dams' performance and associated costs. The obtained results shed light on the interdependencies between dams, the effectiveness of different maintenance strategies, and the cost implications for each configuration. The deterioration trajectories revealed that the presence or absence of downstream dams significantly influenced the deterioration rate of upstream dams. The absence of a downstream dam accelerated the deterioration process, while its presence helped stabilize the upstream dams. Furthermore, the maintenance strategies played a crucial role in managing the dams' condition. Strategies that included preventive maintenance and minor operations resulted in longer periods of satisfactory performance, with dams spending less time in deteriorated states. On the other hand, strategies that relied on major or corrective operations attained higher costs and longer duration in poor or failed states. In addition, it was observed that the presence or absence of upstream and downstream dams had a significant impact on the maintenance costs. In conclusion, this study has contributed to the understanding of check dam deterioration and maintenance strategies in torrent systems. The findings emphasize the importance of considering the inter-dependencies between dams and selecting appropriate maintenance strategies to ensure the longevity and effectiveness of the overall system. From a practical point of view, risk managers understand the importance of timely repairs for critical check dams. This study brings significant value by establishing a robust framework that explicitly incorporates cascading effects into maintenance decision-making. [Integrated with comprehensive real-time data on check dam design, flood forecasts, and geotechnical parameters, it significantly reduces uncertainty for decision-makers, empowering them to make well-informed, evidence-based choices regarding check dam system management and maintenance.](#)

There are several promising avenues for future research. Firstly, this study can be expanded to incorporate a larger number of dams and more complex configurations. Additionally, the inclusion of environmental factors such as climate change could enhance the model's predictive capabilities. Besides, other modes of failures can be considered to model the deterioration of the dam (e.g., aging, internal stability analysis). [Furthermore, the assumption of perfect maintenance operations, while simplifying our analysis, may not consistently reflect real-world scenarios. While this assumption holds for minor maintenance and corrective maintenance, its application to major maintenance can be impractical in engineering contexts. Thus, the consideration of implementing partial renewal maintenance actions offers a more realistic approach.](#) By further exploring the identified research avenues, future studies can make significant advancements in the field, enabling more sustainable and cost-effective management of check dams.

Acknowledgments

This work has been partially supported by MIAI@Grenoble Alpes, (ANR-19-P3IA-0003). We also thank our colleagues from ONF/RTM (French national forest office/Mountain restoration department), particularly Simon Carladous from Directorate for natural risks and Benoit Serra, deputy head of RTM department of Alpes de Haute-Provence, along with their entire team. Their field visits, data provision, and valuable discussions and collaboration have greatly contributed to this project.

References

- Alaswad, S., Xiang, Y., 2017. A review on condition-based maintenance optimization models for stochastically deteriorating system. *Reliability Engineering & System Safety* 157, 54–63. URL: <http://www.sciencedirect.com/science/article/pii/S0951832016303714>.
- Aubry, J.F., Brinzei, N., Mazouni, M.H., 2016. Systems Dependability Assessment: Benefits of Petri Net Models. volume 1 of *Systems and Industrial Engineering Series. Systems Dependability Assessment Set*. ISTE Ltd and John Wiley & Sons Inc.
- Barone, G., Frangopol, D.M., 2014. Life-cycle maintenance of deteriorating structures by multi-objective optimization involving reliability, risk, availability, hazard and cost. *Structural Safety* 48, 40–50. URL: <https://www.sciencedirect.com/science/article/pii/S0167473014000149>, doi:<https://doi.org/10.1016/j.strusafe.2014.02.002>.
- Bernard, 1925. Cours de Restauration des Montagnes. Ecole Nationale des Eaux et Forêts Nancy. [In French].
- Carladous, S., 2017. Approche intégrée d'aide à la décision basée sur la propagation de l'imperfection de l'information—application à l'efficacité des mesures de protection torrentielle. Ph.D. thesis. Ecole des Mines de Saint-Etienne, France. [In French].
- Carladous, S., Tacnet, J.M., Batton-Hubert, M., Dezert, J., Marco, O., 2019. Managing protection in torrential mountain watersheds: A new conceptual integrated decision-aiding framework. *Land Use Policy* 80, 464–479. doi:<https://doi.org/10.1016/j.landusepol.2017.10.040>.
- Chahrour, N., Nasr, M., Tacnet, J.M., Bérenguer, C., 2021. Deterioration modeling and maintenance assessment using physics-informed stochastic petri nets: Application to torrent protection structures. *Reliability Engineering & System Safety* 210, 107524. doi:<https://doi.org/10.1016/j.res.2021.107524>.
- Chahrour, N., Piton, G., Tacnet, J.M., Bérenguer, C., 2022. Designing Protection Systems in Mountains for Reduced Maintenance Costs: Claret's Retention Dam Case Study, in: *Proceedings of the 32nd European Safety and Reliability Conference (ESREL 2022)*, Dublin, Ireland. pp. 2797–2804. doi:10.3850/978-981-18-5183-4_S21-05-576-cd.
- Chen, H.P., Mehrabani, M.B., 2019. Reliability analysis and optimum maintenance of coastal flood defences using probabilistic deterioration modelling. *Reliability Engineering System Safety* 185, 163–174. URL: <https://www.sciencedirect.com/science/article/pii/S0951832018308810>, doi:<https://doi.org/10.1016/j.res.2018.12.021>.
- Cheng, Y., Elsayed, E., Chen, X., 2021. Random multi hazard resilience modeling of engineered systems and critical infrastructure. *Reliability Engineering System Safety* 209, 107453. URL: <https://www.sciencedirect.com/science/article/pii/S0951832021000223>, doi:<https://doi.org/10.1016/j.res.2021.107453>.
- Comiti, F., Lenzi, M.A., Mao, L., 2013. Local scouring at check-dams in mountain rivers, in: Garcia, C.C., Lenzi, M.A. (Eds.), *Check Dams, Morphological Adjustments and Erosion Control in Torrential Streams*. Nova Science Pub Inc, pp. 263–282.
- Couvert, B., Lefebvre, B., Lefort, Ph., Morin, E., 1991. Etude générale sur les seuils de correction torrentielle et les plages de dépôts. *La Houille Blanche* 6, 449–456. doi:10.1051/lhb/1991043ISTEX. [In French].
- Deymier, C., Tacnet, J.M., Mathys, N., 1995. Conception et calcul de barrages de correction torrentielle. Grenoble, France: Cemagref Editions, 287p. [In French].
- Dueñas-Osorio, L., Vemuru, S.M., 2009. Cascading failures in complex infrastructure systems. *Structural Safety* 31, 157–167. URL: <https://www.sciencedirect.com/science/article/pii/S016747300800057X>, doi:<https://doi.org/10.1016/j.strusafe.2008.06.007>ISTEX. Risk Acceptance and Risk Communication.
- Einhorn, B., Eckert, N., Chaix, C., Ravanel, L., Deline, P., Gardent, M., Boudieres, V., Richard, D., Vengeon, J.M., Giraud, G., Schoeneich, P., 2015. Climate change and natural hazards in the alps. *Revue de Géographie Alpine* 103. doi:10.4000/rga.2878.
- Gill, J.C., Malamud, B.D., 2014. Reviewing and visualizing the interactions of natural hazards. *Reviews of Geophysics* 52, 680–722. doi:<https://doi.org/10.1002/2013RG000445>.
- Gill, J.C., Malamud, B.D., 2016. Hazard interactions and interaction networks (cascades) within multi-hazard methodologies. *Earth System Dynamics* 7, 659–679. doi:10.5194/esd-7-659-2016.
- GRIF, 2021. GRIF-Workshop. TOTAL and SATODEV. URL: <https://grif-workshop.fr/>.
- Groupe de travail, 1993. N°93 - 3 TO. Fascicule 62 titre V. Règles techniques de conception et de calcul des fondations des ouvrages de génie civil. Bulletin officiel du Ministère de l'Équipement. Paris, France. [In French].
- Kaplan, E.L., Meier, P., 1958. Nonparametric estimation from incomplete observations. *Journal of the American Statistical Association* 53, 457–481. URL: <http://www.jstor.org/stable/2281868>.
- Laigle, D., 2008. Logichar. <https://forge.irstea.fr/projects/logichar>.
- Li, Y., Dong, Y., Guo, H., 2023. Copula-based multivariate renewal model for life-cycle analysis of civil infrastructure considering multiple dependent deterioration processes. *Reliability Engineering System Safety* 231, 108992. URL: <https://www.sciencedirect.com/science/article/pii/S095183202200607X>, doi:<https://doi.org/10.1016/j.res.2022.108992>.
- Mineo, S., Pappalardo, G., D'Urso, A., Calcaterra, D., 2017. Event tree analysis for rockfall risk assessment along a strategic mountainous transportation route. *Environmental Earth Sciences* 76. doi:10.1007/s12665-017-6958-1.

- 840 Misuri, A., Landucci, G., Cozzani, V., 2021. Assessment of safety barrier performance in the mitigation of domino scenarios caused by natech
841 events. *Reliability Engineering & System Safety* 205, 107278. doi:<https://doi.org/10.1016/j.res.2020.107278>.
- 842 Modarres, M., 1992. *What Every Engineer Should Know about Reliability and Risk Analysis*. CRC Press.
- 843 Morato, P., Papakonstantinou, K., Andriotis, C., Nielsen, J., Rigo, P., 2022. Optimal inspection and maintenance planning for deteriorating
844 structural components through dynamic bayesian networks and markov decision processes. *Structural Safety* 94, 102140. URL: <https://www.sciencedirect.com/science/article/pii/S0167473021000631>, doi:<https://doi.org/10.1016/j.strusafe.2021.102140>.
- 845 Mühlhofer, E., Koks, E.E., Kropf, C.M., Sansavini, G., Bresch, D.N., 2023. A generalized natural hazard risk modelling framework for infrastructure
846 failure cascades. *Reliability Engineering System Safety* 234, 109194. URL: <https://www.sciencedirect.com/science/article/pii/S0951832023001096>, doi:<https://doi.org/10.1016/j.res.2023.109194>.
- 847 ONF-RTM, 2014. *Division Domaniale du torrent de Faucon – Etude de bassin de risques*. Research report V1. Office National des Forêts, Service
848 de Restauration des Terrains en Montagne du Département de Alpes de Haute Provence. [In French].
- 849 Ouyang, M., 2014. Review on modeling and simulation of interdependent critical infrastructure systems. *Reliability Engineering System Safety* 121,
850 43–60. URL: <https://www.sciencedirect.com/science/article/pii/S0951832013002056>, doi:<https://doi.org/10.1016/j.res.2013.06.040>.
- 851 Pescaroli, G., Alexander, D., 2016. Critical infrastructure, panarchies and the vulnerability paths of cascading disasters. *Nat Hazards* 82, 175–192.
852 doi:10.1007/s11069-016-2186-3.
- 853 Piton, G., Carladous, S., Recking, A., Tacnet, J.M., Liébault, F., Kuss, D., Queffélec, Y., Marco, O., 2017. Why do we build check dams in
854 Alpine streams? An historical perspective from the French experience. *Earth Surface Processes and Landforms* 42, 91–108. doi:<https://doi.org/10.1002/esp.3967>.
- 855 Pol, J.C., Kindermann, P., van der Krogt, M.G., van Bergeijk, V.M., Remmerswaal, G., Kanning, W., Jonkman, S.N., Kok, M., 2023. The effect of
856 interactions between failure mechanisms on the reliability of flood defenses. *Reliability Engineering & System Safety* 231, 108987. URL: <https://www.sciencedirect.com/science/article/pii/S0951832022006020>, doi:<https://doi.org/10.1016/j.res.2022.108987>.
- 857 Prendergast, L.J., Gavin, K., 2014. A review of bridge scour monitoring techniques. *Journal of Rock Mechanics and Geotechnical Engineering* 6,
858 138 – 149. doi:<https://doi.org/10.1016/j.jrmge.2014.01.007>.
- 859 Recking, A., Degoutte, G., Camenen, B., Frey, P., 2013. *Hydraulique et transport solide*, in: Recking, A., Richard, D., Degoutte, G. (Eds.), *Torrents
860 et rivières de montagne : Dynamique et aménagement*. Editions Quae, Paris, France. [In French].
- 861 Rinaldi, S.M., Peerenboom, J.P., Kelly, T.K., 2001. Identifying, understanding, and analyzing critical infrastructure interdependencies. *IEEE Control
862 Systems Magazine* 21, 11–25. doi:10.1109/37.969131. cited By 1332.
- 863 Saleh, A., Chiachío, M., Salas, J.F., Kolios, A., 2023. Self-adaptive optimized maintenance of offshore wind turbines by intelligent petri nets. *Relia-
864 bility Engineering System Safety* 231, 109013. URL: <https://www.sciencedirect.com/science/article/pii/S0951832022006287>,
865 doi:<https://doi.org/10.1016/j.res.2022.109013>.
- 866 Sharma, N., Gardoni, P., 2022. Mathematical modeling of interdependent infrastructure: An object-oriented approach for generalized network-
867 system analysis. *Reliability Engineering System Safety* 217, 108042. URL: <https://www.sciencedirect.com/science/article/pii/S0951832021005470>, doi:<https://doi.org/10.1016/j.res.2021.108042>.
- 868 Surell, A., 1841. *Étude sur les torrents des Hautes-Alpes*. Carilian-Goeury. [In French].
- 869 Tacnet, J.M., Degoutte, G., 2013. *Torrents et rivières de montagne : Dynamique et aménagement*. A. Recking, D. Richard, G. Degoutte. Paris,
870 France : Quae. Chap. 5, p. 267 - 331.. chapter Principes de conception des ouvrages de protection contre les risque torrentiels.
- 871 Vieira, M., Henriques, E., Snyder, B., Reis, L., 2022. Insights on the impact of structural health monitoring systems on the operation and maintenance
872 of offshore wind support structures. *Structural Safety* 94, 102154. URL: <https://www.sciencedirect.com/science/article/pii/S0167473021000771>, doi:<https://doi.org/10.1016/j.strusafe.2021.102154>.
- 873 Zhao, Y., Cai, B., Kang, H.H.S., Liu, Y., 2023. Cascading failure analysis of multistate loading dependent systems with application in an overloading
874 piping network. *Reliability Engineering & System Safety* 231, 109007. URL: <https://www.sciencedirect.com/science/article/pii/S0951832022006226>, doi:<https://doi.org/10.1016/j.res.2022.109007>.